Wind-driven upwelling on the Western Agulhas Bank: A study using ERA5 and WASA3 winds

Giovanna Lara Birkett

Dissertation presented in partial fulfilment of the requirements for the degree of Master of Science in the Department of Oceanography

University of Cape Town

February 2023

Supervisors:

Prof Juliet Hermes

Dr Jennifer Veitch

Mr Matthew Carr

Plagiarism Declaration

I, Giovanna Lara Birkett, hereby declare that this thesis is my own, original work unless otherwise indicated in the form of referencings and citings. I have used the Harvard Referencing system to identify every idea mentioned in my thesis that was not my own and have attributed it to the original author/s. I also will ensure that neither fractions of, nor this entire thesis has been, is being or will be used by another party with the intention of claiming it being their own work.

Signature: Signed by candidate

Date: 12 February 2023

Acknowledgements

This thesis was made possible by the guidance and support of my incredible supervisors. Juliet, Jenny and Matt, thank you for all you have taught me throughout the past year and for inspiring my passion in this topic. It has been an honour to work with and learn from such an amazing team.

Thank you to the lecturers who have taught me throughout the past year, and to the academics in MARiS for organising this course. I have learnt invaluable skills that will benefit me in my future career. I am also thankful to my classmates for the support and for keeping me motivated throughout this degree.

I am thankful for the funding received from the South African Environmental Observation Network (SAEON).

Finally, thank you to my family, who are the reason I have the opportunity to complete my Masters degree, and who have been supportive throughout the entire process.

Abstract

The Southern Benguela Upwelling System (SBUS), located along the west coast of South Africa, is unique in that it is the only eastern boundary upwelling system bounded at both ends by warm water masses, and with no continental boundary between it and the adjacent western boundary current, the Agulhas Current. The Western Agulhas Bank (WAB), defined as the region over the Agulhas Bank from Cape Point to Cape Agulhas, is the southernmost region of the SBUS however it has a markedly different coastline orientation, and upwelling dynamics in this region are understudied. This study compares two different modelled wind products, ERA5 (31 km resolution) and WASA3 (3.33 km resolution), assessing coastal wind-driven upwelling in the WAB. Wind-driven upwelling, derived from the higher resolution WASA3 dataset is used to identify and investigate the seasonality of three discrete regions of upwelling within the WAB. WASA3 is shown to capture stronger orography-induced wind stress curl which drives the locations of upwelling cells and contributes 67.23% to the total upwelling velocity observed at Cape Hangklip in January, just more than double the contribution of alongshore wind stress driven Ekman pumping. Theoretical wind-driven upwelling in Cape Hangklip is shown to be stronger than in the Cape Peninsula upwelling cell in January, despite previous literature describing the Cape Peninsula as a stronger upwelling cell. This indicates that other factors not accounted for in this study likely suppress upwelling at Cape Hangklip, such as shallow bathymetry and stratification. The study highlights the importance of using a high-resolution wind product to resolve small scale features, emphasising that numerical models using low resolution wind products such as ERA5 should be used with caution when interpreting simulated upwelling velocities. Given the socio-economic importance of the WAB, and the effect of the upwelling on aquaculture, fishing and tourism in this region, it is suggested that WASA3 or a similar high resolution wind dataset is used to force numerical models with the aim of gaining a greater understanding of the upwelling dynamics in this region.

Table of Contents

List of Figures

List of Tables

1. Introduction

The Western Agulhas Bank (WAB), defined as the oceanic region over the western half of the Agulhas Bank, from Cape Point to Cape Agulhas (Figure 2.1; Largier et al., 1992), constitutes the southernmost region of the Southern Benguela Upwelling System (SBUS). This region is unique in that it is the only eastern boundary upwelling system (EBUS) with a termination of the continent so far equatorward, providing an opportunity to study the transitional region between the EBUS on the west coast, and the warm western boundary system on the east coast, being the Agulhas Current system (Hutchings et al., 2009; Shillington et al., 2006). While this region is defined as being part of the SBUS, it differs in many ways, such as the orientation of the coastline being more zonally oriented compared to the north-south orientation characteristic of EBUSs. The region also has many bays and headlands, with the possibility to greatly influence the upwelling dynamics through orography-induced modification of the wind. Upwelling, a key feature of west coast regions driving primary productivity in EBUSs (Chavez and Messié, 2009), has been well studied along the coast in the SBUS from Lüderitz to Cape Point, however substantially less work has been done to understand upwelling on the WAB, despite it being of great socio-economic importance.

Previous studies in the WAB report upwelling to occur downwind of prominent headlands due to the input of negative wind stress curl, at Cape Hangklip, Cape Point and Cape Agulhas (Boyd et al., 1985; Coleman et al., 2021; Cram, 1970; Dufois and Rouault, 2012; Jury, 1984; Jury, 1988; Largier et al., 1992). Of these studies, *in situ* measurements have been sparse and have not been carried out over sufficient time periods or across all seasons. Most upwelling studies in the WAB have focused on spring and summer, as this is the upwelling season which has effects on fish spawning (Largier et al., 1992), however this does not allow for a complete understanding of the seasonal cycle of upwelling in this region. Satellite sea surface temperature (SST) has been used as a proxy for upwelling, however large inaccuracies in satellite SST are seen at upwelling cells (Carr et al., 2021), and other factors impact the SST in these regions, indicating that this method is unsuitable to study upwelling on the WAB.

There are complex interactions between upwelling and wind in the SBUS and WAB, and past modelling studies in the WAB are limited by coarse resolution wind products, resulting in misrepresentation of upwelling dynamics (Small et al., 2015). There is limited work done on assessing the effects of a spatially varying wind field in the WAB (Coleman, 2019), which has been shown to significantly affect upwelling. By gaining a better understanding of the two mechanisms of wind-driven upwelling, through alongshore wind stress and wind stress curl, this information can be incorporated into numerical ocean models aimed at simulating the upwelling dynamics of the region. In order to gain this understanding, a high-resolution wind dataset is needed to capture the small-scale variations in wind around the coast (Abrahams et al., 2021).

Gaining a complete understanding of upwelling in the WAB is important as it is home to many species of marine animals. There are many residential areas along the coast of the WAB, with people reliant upon this region for small-scale fishing, recreation and ecotourism (Nicholson, 2012). The conditions on the WAB during the upwelling season likely play a major role in the success of spawning of fish species such as anchovies (Jury, 1988; Largier et al., 1992). Fisheries in this region such as in Walker Bay have been in decline due to overexploitation (Attwood and Farquhar, 1999). Given that upwelling in this region supports primary production and the base of the food chain, it is vital that the processes behind the upwelling are understood so that better management and planning of the fisheries can occur during the future to prevent further collapse. Shifts in fish species could also have effects on ecotourism in the area, such as shark cage diving.

There are also aquaculture farms along the coast in this region, such as abalone farms in Walker Bay, Hermanus and Gansbaai (Ponton, 2021). Changes in upwelling and thus changes in the nutrient contents and temperature of the water at the coast that is fed into the aquaculture farms may significantly impact the success of the aquaculture.

It is vital that upwelling in this region is studied as, in the face of changing global wind patterns, upwelling is predicted to expand southwards over this region as has already been observed over the Agulhas Bank (Lamont et al., 2018), with areas such as False Bay becoming increasingly similar to the rest of the EBUS. This predicted intensification in the upwelling

already occurring in this area would result in shifts in pelagic populations, which can have large socio-ecological effects (Pfaff et al., 2019). This thesis forms the first step to gaining an improved understanding of wind-driven upwelling on the WAB necessary to be able to hypothesise as to how changes in global wind patterns in the future might impact this region.

This study seeks to gain an improved understanding of the mechanisms of wind-driven upwelling in the WAB. It does this by assessing the impact of a high-resolution wind product, WASA3, on theoretical wind-driven upwelling along the coast compared to a commonly used low-resolution wind product, ERA5. This is done through calculation of wind-driven upwelling related variables; namely wind stress, alongshore wind stress, wind stress curl and upwelling velocities based on these. In doing so, this study aims to analyse the coastline of the WAB to identify regions where upwelling is expected to occur. From this, this study aims to classify the seasonality of wind stress curl and alongshore wind stress driven upwelling in these regions. In doing so, this study becomes one of the first to analyse upwelling along the entire coastline of the WAB using a wind product of such high resolution, providing a complete description of wind-driven upwelling mechanisms and region where upwelling is expected to occur.

2. Literature Review

2.1 An overview of the Benguela Current System

The Benguela Current is the broad eastern boundary current of the South Atlantic, flowing northwards along the western coast of southwestern Africa (Figure 2.1). This current forms the eastern limb of the South Atlantic subtropical gyre (Garzoli and Gordan, 1996), and is one of the four main eastern boundary currents in the world's oceans, along with the California Current, the Peru Current and the Canary Current (Shannon and Nelson, 1996). The Benguela and other eastern boundary currents advect cold water from the high latitudes to the low latitudes and are associated with wind-driven upwelling of cold, nutrient rich water at the coast inshore of the current (Philander and Yoon, 1982; Rossi et al., 2009; Shannon, 2001). EBUSs are the most productive areas in the world's oceans, supporting up to 20% of global fish catches despite only accounting for less than 1% of the total ocean area (Pauly and Christensen, 1995).

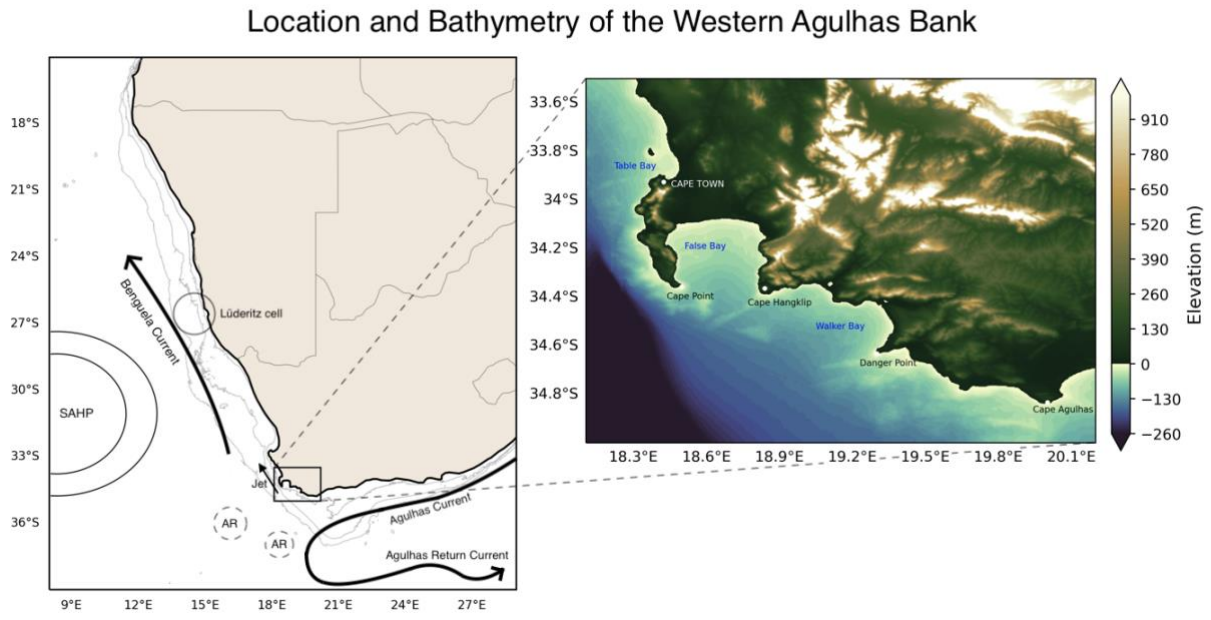

Figure 2.1: Location and bathymetry of the Western Agulhas Bank (WAB). The Agulhas Current, Benguela Current, Agulhas Return Current, Agulhas leakage through Agulhas rings (AR), wind jet, South Atlantic High Pressure (SAHP), and Lüderitz upwelling cell are annotated, with the 100, 200 and 1000 m depth contours shown. The study region of this thesis is highlighted by the black box and the bathymetry and topography of this region are plotted using data from GEBCO.

The Benguela Current is unique as it is not only influenced by a tropical warm water regime at its equatorward boundary at the Angola-Benguela Front, but also at its poleward via interactions with the Agulhas Current. This arises due to the termination of the African continent more equatorward than the continents associated with the other EBUSs, creating an interesting transitional region between the Benguela and Agulhas Current Systems (Hutchings et al., 2009; Shillington et al., 2006). There are different definitions of the boundaries of the Benguela Current System. It is becoming increasingly recognized that the upwelling extends southward as far as Cape Agulhas, and therefore this thesis defines the Benguela region as extending from the northern boundary at the Angola Benguela Front south until Cape Agulhas, as done by Abrahams et al. (2021).

In the Benguela Upwelling System, the wind regime is controlled by the presence of the South Atlantic High Pressure (SAHP) system, the seasonal pressure field over the continent, and the eastward moving cyclones that affect the southern part of Africa (Shannon, 2001). The SAHP is an anticyclonic circulation that shifts seasonally over 6° of latitude, moving equatorward in austral winter and southward in austral summer (Hutchings et al., 2009; Shannon, 2001; Shannon and Nelson, 1996). In summer, winds tend to be alongshore in the Benguela due to the coastal plain acting as a barrier, and flow in a southerly direction due to the anti-cyclonic rotation of the SAHP (Shannon, 2001).

Upwelling, and the surfacing of cold, nutrient rich water from below, drives primary productivity in EBUSs (Chavez and Messié, 2009). Upwelling in the Benguela and other EBUSs is predominantly caused by the offshore Ekman transport of surface water along the coast due to alongshore, equatorward winds, which results in an upward flux of water toward the surface to replace the displaced water (Bakun, 1973). Water is transported offshore to the left (right) of winds in the Southern (Northern) Hemisphere (Largier, 2020; Nelson and Hutchings, 1983). Water at depth tends to have higher nutrient concentrations due to decomposition of organic matter as well as higher concentrations of CO_2, lower pHs and lower concentrations of dissolved oxygen (Chavez et al., 2018). Upwelling of this water along the coast provides a source of nutrients and supports phytoplankton growth and high levels of productivity characteristic of EBUSs (Largier, 2020).

Upwelling along the coast is also affected by Ekman pumping that is caused by a shear in the wind field (Philander and Yoon, 1982). Wind stress curl is the measure of wind shear and tends to be negative (positive) along Southern Hemisphere (Northern Hemisphere) eastern boundaries as a result of the rotation and drop off of alongshore winds toward the coast due to the effect of friction with the land boundary (Capet et al., 2004). In the Southern Hemisphere, negative wind stress curl induces upward Ekman pumping which causes the uplift of water from below, contributing to upwelling and forming a significant source of nutrients (Rykaczewski and Checkley Jr., 2008). High values of wind stress curl occur downstream of headlands in the Benguela and together with Ekman transport, determine the upwelling processes of the area (Bentamy et al., 2021). This orography-induced wind stress curl occurs at fine spatial scales, and thus high-resolution wind products are needed to properly quantify the effect of this wind stress curl on upwelling (Capet et al., 2004; Desbiolles et al., 2014).

Upwelling in the Benguela is concentrated at several upwelling cells typically located at areas of cyclonic wind stress curl, inducing upward Ekman pumping (Bentamy et al., 2021) and where there is a change in orientation of the coastline (Shannon and Nelson, 1996). The Lüderitz cell, situated at 27 °S, experiences the strongest upwelling throughout the year, and divides the Benguela into two distinct regions, the Northern Benguela Upwelling System (NBUS) and the SBUS (Veitch et al., 2009). The NBUS consists of the Cunene, Namibia and Walvis Bay upwelling cells. In the SBUS, upwelling is concentrated at the Namaqua, Columbine, Cape Peninsula and the Agulhas upwelling cells (Lutjeharms and Meeuwis, 1987).

Winds in the NBUS show less seasonality, due to the position of the SAHP over this region for most of the year creating strong alongshore upwelling favourable winds, resulting in perennial upwelling, and associated higher phytoplankton biomass (Hutchings et al., 2009; Pitcher et al., 1992). In the SBUS the seasonal shift in the position of the SAHP results in a larger seasonality in the winds. In summer, winds are predominantly southerly to south-easterly, along the coast, making summer the main upwelling season in this region. During spring, summer and autumn the periodic ridging of the SAHP eastwards causes sustained south-easterly winds. This process typically causes periods of four to five days of strong south

easterlies with velocities of 18-25 m s^{-1} causing periodic rather than sustained upwelling, however there are occasions where this can persist for up to twelve days. During winter, cyclones with characteristic low-pressure centres move west to east across the southern region of the African continent, and cause predominantly north-westerly winds, not favourable of upwelling, however winds during winter are much more variable than those during summer (Andrews and Hutchings, 1980; Shannon and Nelson, 1996).

2.2 The Western Agulhas Bank

The Western Agulhas Bank (WAB), defined as the oceanic region over the western half of the Agulhas Bank (>200m depth) from Cape Point to Cape Agulhas (Figure 2.1; Boyd et al., 1985; Largier et al., 1992), constitutes the southernmost extent of the SBUS. The separation of the WAB and the Eastern Agulhas Bank (EAB) to the east of Cape Agulhas is evident by the regional differences in chemical and biological indicators such as oxygen concentration, phytoplankton distributions (Largier et al., 1992), and a rapid change in intertidal flora and fauna across this boundary as observed by Christensen (1980). This difference between these regions has been attributed to their respective distances from the Agulhas Current, with the EAB being in closer proximity to the Agulhas, as well as angle of the coastline in relation to winds that cause upwelling (Largier et al., 1992).

While the WAB is often classified as part of the SBUS, it differs in many ways to the rest of the region, and it has been suggested that a transition in oceanic conditions occurs at Cape Point (Andrews and Hutchings 1980; Bang, 1973), indicating a difference between these two areas of the SBUS. The WAB has a markedly different coastline orientation (Figure 2.1; Jury, 1988) and has bays and headlands, unlike the rest of the SBUS. The WAB also has a very wide continental shelf in comparison to the narrow shelf off the west of Cape Point (Boyd et al., 1985). While the WAB forms part of the SBUS on the west coast, the outer continental shelf of this region is influenced by the Agulhas Current through the proximity of the Agulhas Retroflection and Agulhas Leakage, creating a highly dynamic and complex oceanic region at the transition between an EBUS and a western boundary current system (Largier et al., 1992; Biastoch et al., 2008). The uniqueness of this transitional region creates localised upwelling regimes that are largely understudied.

2.2.1 Winds on the WAB

During summer, the general wind regime over the WAB consists of predominantly south-easterly winds as a result of the southerly position of the SAHP. The winds generally follow the angle of the coast, with slight onshore components along the coastal region of the WAB compared to a more longshore flow on the west coast around the Cape Peninsula (Boyd et al., 1985). During summer, but particularly between October and December, periods of intense south-easterly 'blows' occur for four to six days when the SAHP ridges around the continent (Wainman et al., 1987). These periods are followed by periods of weaker and shallower south-easterly winds (Coleman et al., 2021). Sustained periods of upwelling favourable winds are needed to cause offshore movement of surface water and upwell water from below. During winter, the winds are much more variable with north-westerly winds dominating, although with shorter durations than the periods of strong south-easterlies during summer. These winds occur due to the cyclonic low pressure systems that originate in the subantarctic region moving east over the WAB and the continent during winter (Boyd et al., 1985).

2.2.2 Upwelling on the WAB

Upwelling in the Southern Benguela occurs regularly in summer, whereas the upwelling over the WAB is far more transient and episodic (Largier et al., 1992). Upwelling occurs along the WAB during summer months, as a result of the predominantly south-easterly wind directions and offshore Ekman transport of water, as well as complex interactions with the coastline and bathymetry (Largier et al, 1992). Boyd et al. (1985) found uplift of cold subsurface water in the WAB in months where south-easterly winds were dominant, during 12 monthly cruises throughout the year, however only in some of these months did upwelling reach the surface. Largier et al. (1992) report that upwelling in the WAB occurs on short time scales of 2-4 days.

The transient nature of the upwelling within the WAB relative to rest of the SBUS require that winds need to blow over a longer time period in order to observed an upwelling signal through SST at the surface. During summer, the water in the WAB is more stratified than in winter (Largier et al., 1992), and the response of upwelling to wind is slower than that off the west

of Cape Peninsula. Stratification of the water column plays an important role in upwelling, with increased stratification on the WAB preventing cold, upwelled waters from reaching the surface. Stratification of the water column increases into the summer, with a strong thermocline and temperature difference between the warm surface layers and cold layers at depth (Coleman et al., 2021). Upwelling in the WAB also seems to be less responsive to south-easterly winds possibly because the winds tend to have stronger onshore components in this region compared to the rest of the Southern Benguela (Boyd et al., 1985). Another factor that could contribute to the observed decreased upwelling response of the WAB is the shallow, gentle bathymetry making source waters for upwelling less available and frictionally retarding pulses of upwelling (Boyd et al., 1985). The effect of friction on retarding upwelling would increase towards the east on the WAB (Boyd et al., 1985). Off Cape Peninsula the steep bathymetry causes cold, nutrient rich waters to be readily available to be upwelled in this zone. The presence of sub-marine canyons off Cape Point and Cape Columbine, both part of the southern Benguela, likely channels cold subsurface water to the region enhancing the availability of water for upwelling (Abrahams et al., 2021; Boyd et al., 1985; Chapman and Largier, 1989; Nelson, 1981).

2.3 Sub-regions of the WAB

2.3.1 False Bay

False Bay is the largest natural bay along the South African coast and has complex wind and upwelling structures as a result of the surrounding mountain ranges (Figure 2.1; Coleman et al., 2021). The Cape Peninsula mountains flank the bay to the west and the Hottentots-Holland mountains to the east that extend down to Cape Hangklip with elevations greater than 1000m (Coleman, 2019; Jury, 2020). To the north of the bay, the Cape Flats are a flat, sandy region that connect the mountains to the west and east (Coleman, 2019). The bay is less than 100m deep, with an estimated average depth of about 50m (Nicholson, 2012).

Upwelling in False Bay occurs during summer, as a result of the interaction of the predominant winds and the headlands of the bay (Largier, 2020). The summer southeasterlies that occur over the WAB are predominantly shallow, not extending higher than the Cape Hangklip and Cape Point mountains, and are thus diverted around the mountains. This diversion causes

acceleration across False Bay as they flow around these capes, forming a low-level wind jet across the bay in summer. The formation of the jet is attributed to the orographic channelling of wind as well as the vertical constraint by the trade wind inversion and the sinking of air due to loss of sensible heat (Jury, 2020). South-easterly winds with components parallel to the shore cause upwelling in this region due the offshore Ekman transport of water. The channelling of this wind by the Cape Hangklip and Cape Point mountains forms a wind shadow on the leeward side of these mountains (Largier, 2020; Wainman et al., 1987), as well cyclonic vorticity (negative wind stress curl) in the wind to the west of these capes. This input of cyclonic vorticity enhances upwelling to the west of the capes (Jury, 2020; Nelson, 1981). The Cape Hangklip mountain range is higher than the Cape Point mountains and therefore creates a stronger wind shadow and stronger diversion of the wind around Cape Hangklip than around Cape Point (Coleman et al., 2021). Summer is the main upwelling season in this region, as in winter, deep north-westerly winds extending higher into the atmosphere and more variation in wind direction do not promote upwelling. The effect of orography on winds in winter is also lessened as these winds tend to be deeper than winds in summer (Jury, 1988).

False Bay has been classified as a 'upwelling-trap bay' as upwelling waters are held in the bay through wind flowing into the bay as a result of the influence of the Cape Hangklip and Cape Peninsula mountains (Largier, 2020). This may increase productivity of the bay as nutrient rich upwelled waters are trapped in the bay allowing for photosynthesis and phytoplankton growth (Largier, 2020). This process of wind flow into the bay may however create localised downwelling, if the water column is not strongly stratified (Largier, 2020).

During summertime (October to April) periods of upwelling of cold (10.2 - 12 C), nutrient rich water to the west of Cape Hangklip (Jury, 1984) have been observed in surveys during strong south-easterly winds (Cram, 1970), in model output (Coleman et al., 2021) and by a combination of sea surface temperature (SST) satellite products and *in situ* temperature and wind measurements (Dufois and Rouault, 2012). Prevailing south-easterly winds over this region cause the cooler upwelled water to drift into the centre of False Bay, compared to the warmer waters on the north-eastern coast in the wind shadow created by the Cape Hangklip mountains (Cram, 1970; Jury, 2020). It has also been suggested that an 'upwelling shadow' exists in False Bay. An upwelling shadow refers to the slow circulation of water in a bay during

periods of upwelling, detected by warmer waters in this region (Graham and Largier, 1997). During periods of south-easterly winds, an anticyclonic circulation has been shown to occur off Gordon's Bay in the north-eastern region of False Bay (Coleman et al., 2021). It is possible that this is the upwelling shadow suggested to occur in False Bay by Graham and Largier (1997).

Jury (2020) postulate that upwelling occurs in pulses in early summer, with quiescent spells in late summer, however Boyd et al. (1985) report upwelling to occur most in late summer, particularly between February and April. Largier et al. (1992) report that upwelling occurs earlier off Cape Point than off the coast in the WAB as upwelling in the WAB requires the SAHP to be far enough south to ridge around the continent, creating the south-easterly winds that drive upwelling over this region and therefore is strongest in February-March, however, can occur as early as November or as late as April. The ridging of the SAHP is not permanent and is the reason behind the episodic nature of the upwelling on the WAB, in contrast to the more regular upwelling in the rest of the Southern Benguela (Largier et al., 1992).

2.3.2 Walker Bay

Walker Bay, to the east of False Bay, is a smaller, more open bay downstream of Danger Point. Similarly to False Bay, Walker Bay is flanked by mountains to the east, however these are not as high as the Cape Hangklip mountains (Jury, 1988). Upwelling has been noted in Walker Bay, to the west of Danger Point (Boyd et al., 1985; Dufois and Rouault, 2012; Jury, 1988; Largier et al., 1992) and has been shown to support photosynthesis and biodiversity upon which people are dependent for food (Attwood and Farquhar, 1999). Upwelling off the west side of Danger point occurs during periods of sustained south-easterly wind as a result of orographic channelling of this cape (Boyd et al., 1985; Dufois and Rouault, 2012). It is likely that stronger south-easterly winds are needed to cause upwelling off Danger Point, such as those occurring during the ridging of the SAHP (Jury, 1988) and therefore the upwelling here is less sensitive than that occurring to the west of Cape Hangklip. The relative lower mountains do not extend as close to the coast as for Cape Hangklip, and therefore the channelling of the wind, orography-induced wind stress curl and resultant upwelling is not as strong or frequent (Jury, 1988).

2.3.3 Cape Agulhas

Upwelling has also been shown to occur to the west of Cape Agulhas periodically in summer in both satellite imagery and *in situ* measurements (Dufois and Rouault, 2012; Largier et al., 1992), however to a lesser extent than that off Danger Point due to the even lower coastal orography and further reduced channelling of the wind and orography-induced wind stress curl (Jury, 1988; Largier et al., 1992). Upwelling favourable winds in this region have a stronger easterly component compared with the rest of the WAB due to the change in orientation of the coastline around Cape Agulhas, and these winds have been shown to occur irregularly during summer causing periods of upwelling (Jury, 1988).

3. Data and Methods

3.1 Data

In this study, two wind products, ERA5 and WASA3, are compared for the SBUS and along the WAB by calculating upwelling relevant variables. The WAB is defined as the coastal region from Cape Point to Cape Agulhas off the South African south coast, however, the following analysis included the coastal regions east of Cape Agulhas and north of Table Bay, in order to include the Cape Peninsula upwelling cell. This well-defined cell does not form part of the WAB but was selected to be included in analysis to provide a comparison to the upwelling cells on the WAB. From this analysis, WASA3 is selected to study the seasonality of three upwelling cells identified along the coast, namely the Cape Peninsula, Cape Hangklip and Danger Point upwelling cells. Below is an outline of the datasets used in this study, followed by the methodology used to study upwelling in this region.

3.1.1 ERA5

Wind data from ERA5 reanalysis (Hersbach et al., 2018) is used in this study to calculate the resultant upwelling velocities along the coast of the WAB (Figure 2.1). ERA5 is produced by the European Centre for Medium-Range Weather Forecasts (ECMWF) using historical observations combined with the Integrated Forecasting System (IFS) Cy41r2 model to produce estimates of atmospheric, land and oceanic variables. The ERA5 dataset is produced on reduced Gaussian grids, such that the distance between grid points is approximately constant (Olauson, 2018). ERA5 has a global spatial domain, with a horizontal resolution of 31 km, compared to its predecessor, ERA-Interim with a resolution of 80 km (Bell et al., 2021; Hersbach et al., 2020). The ERA5 dataset has an hourly temporal resolution over the period from 1950 until present (Olauson, 2018). In this study, the zonal wind at 10 m above sea level was used for a spatial domain covering the oceanic region around South Africa, over the period from 1991 to the end of 2019.

3.1.2 WASA3

Phase 3 of the Wind Atlas of South Africa (WASA3) Project (Hahmann et al., 2021) is a regional wind dataset for South Africa and the surrounding ocean region generated using the Weather Research & Forecasting Model (WRF) (Skamarock et al., 2008) using a Lambert conformal grid projection. The model uses a triple nested domain, with the innermost domain having a horizontal resolution of 3.33 km. The model is forced using ERA5 wind and wind speeds and directions, with a temporal resolution of 30 minutes. In this study, WASA3 wind data at 10 m above sea level was used with an hourly time step from 1991 to the end of 2019.

WASA3 is an updated version of the WASA2 wind product (Hahmann et al., 2018), however with a more suitable WRF model configuration and a new, more accurate method of downscaling the WRF-derived wind climate. WASA3 at the time of release was the most extensive wind climatology for South Africa (Hahmann et al., 2021). WASA3 has been validated extensively over land and has been compared to measured winds from wind masts (Hahmann et al., 2021) however in this study it is being used over the coastal ocean. While WASA3 has not been validated over the ocean, WASA2 has been validated over several sites around False Bay by Coleman et al. (2021), namely Cape Town International Airport, Strand, Roman Rock and Cape Point. The validations showed that generally the WASA data was in agreement with measurements and was deemed acceptable for use in the oceanographic study in this thesis (Coleman et al., 2021).

3.1.3 OSTIA

In addition to the two wind products being studied in this thesis, SST data from the Operational Sea Surface Temperature and Ice Analysis (OSTIA) system (Good et al., 2020; https://doi.org/10.48670/moi-00168) is used to provide an overview of upwelling processes around the South African west coast. OSTIA generates Level 4 SST and sea ice datasets from satellite data and *in situ* observations, at a global scale. The data has a daily temporal resolution and is available from 1 October 1981 to present, with a spatial resolution of 0.05 degrees (roughly 5 km). For this study, SST data has been used from 1991 to the end of 2019, the same period as the data studied from ERA5 and WASA3. The data has been extracted for the same spatial domain as the wind datasets.

3.2 Methods

In order to study the wind and resultant upwelling over the WAB, monthly climatologies of wind speed from the ERA5, WASA3 and OSTIA datasets were created. From this, wind stress was plotted from ERA5 and WASA3 for all months (Appendix A); January and July were shown to be representative of austral summer and winter respectively and were thus selected to be used in further analysis. From here on out, summer (winter) will be used to refer to January (July).

3.2.1 Wind stress

In order to investigate wind-driven upwelling on the WAB and surrounds, wind stress was calculated from the ERA5 and WASA3 wind speed climatologies over the entire domain (Eq.1). τ_x and τ_y refer to the zonal and meridional components of the wind stress vector, ρ_A refers to the density of air, C_D refers to the drag coefficient taken as a constant 0.0015, u_{10} and v_{10} refer to the wind speed at 10 m above sea level in the zonal and meridional directions respectively and wspd refers to the wind speed (Eq.2).

$$(\tau_x, \tau_y) = \rho_A \, C_D(u_{10}, v_{10}) \, wspd \qquad (1)$$

$$wspd = \sqrt{{u_{10}}^2 + {v_{10}}^2} \qquad (2)$$

3.2.2 Wind Stress Curl

Having calculated the wind stress, the wind stress curl was calculated from the wind stress climatologies to further investigate the wind-driven upwelling (Eq.3). The change in zonal wind stress ($\delta\tau_x$) divided by the distance between meridional grid points (δy) is subtracted from the change in meridional wind stress ($\delta\tau_y$) over the distance between zonal grid points (δx). Wind stress curl results in Ekman pumping in the ocean, which causes either a positive or negative vertical velocity of water that acts to enhance or suppress upwelling, respectively.

$$wsc = \frac{\partial \tau_y}{\partial x} - \frac{\partial \tau_x}{\partial y} \qquad (3)$$

Next, ERA5 was regridded onto the WASA3 domain, through interpolating bilinearly, using the xESMF Python package. The difference between WASA3 and ERA5 wind stress curl was calculated using interpolated ERA5 wind stress curl due to the differences in horizontal grid resolution. These plots allow us to investigate the ability of each dataset to capture wind stress curl over the region, as it has a large control on where upwelling will occur.

3.2.3 Alongshore Wind Stress

Alongshore wind stress was calculated for the interpolated ERA5 climatology and the WASA3 climatology, as it results in offshore Ekman transport and thus vertical velocities at the coast that either enhance or suppress upwelling. The data points at 0 m depth (i.e. the coast) were identified to extract the wind stress at the coastline. The wind stress vectors were then rotated along the coastline to obtain alongshore wind stress such that positive values represent an upwelling favourable wind stress and negative values represent downwelling favourable wind stress. The difference between WASA3 and ERA5 alongshore wind stress was calculated. The wind data for both products was also resampled daily from which the standard deviation in alongshore wind was calculated (Eq.4). σ is the standard deviation, x_i is each daily average value of alongshore wind at the coast for all days in January or July, μ_m is the monthly climatology for any month m, in this case the climatology of alongshore wind for January and July and N_m is the total number of days corresponding to month m. The standard deviation is calculated to give an idea of the intraseasonal and interannual variability in wind strength at the coastline within January and July. The alongshore wind stress was investigated for January and July, over a smaller spatial domain to pick out the finer-scale spatial details and potential seasonal differences within the region.

$$\sigma = \sqrt{\frac{\sum(x_i - \mu_m)^2}{N_m}} \qquad (4)$$

3.2.4 Upwelling Velocity

Theoretical wind-driven upwelling velocities were calculated for ERA5 and WASA3 January and July climatologies, according to the following methods:

i) Bakun Upwelling Index

Alongshore wind stress with the coast on the right of the wind (defined as positive in this thesis) results in movement of water offshore in the Southern Hemisphere, termed Ekman transport. The Bakun Upwelling Index (BUI) represents the magnitude of the offshore component of Ekman transport, which is used as an indication of the strength of upwelling of water to replace the water displaced at the surface (Bakun, 1973). In this study, the offshore Ekman transport as a result of alongshore wind stress, $U_{E,acs}$, was calculated (Eq. 5), whereby τ_{als} is the alongshore wind stress, ρ_o is the density of seawater and f is the Coriolis parameter at each latitude. Negative values show transport directed offshore, according to the convention chosen in this thesis.

$$U_{E,acs} = \frac{\tau_{als}}{\rho_{of}} \qquad (5)$$

Instead of using the BUI as described above as an indication of upwelling strength, upwelling velocities were calculated from the BUI by dividing the transport by a length scale over which upwelling occurs. This was set to be 20 km as, in evaluation of model output from the Regional Ocean Modelling System (ROMS) (Tedesco et al., 2019) in the Benguela Region, upwelling occurs over roughly 20 km off the coast. While there are other methods of selecting this length scale, such as using the Rossby radius of deformation, 20 km was deemed most appropriate in this study. This is consistent with the Rossby radius of deformation computed for this region by Chelton et al. (1998) of 20 to 30 km. The result of this calculation is a theoretical upwelling velocity as a result of alongshore wind stress, which in this study shall be referred to as “BUI” for simplicity.

ii) Ekman Pumping

To obtain the resultant upwelling velocities from wind stress curl at the coast, values of wind stress curl were extracted for the same coastal indices identified above for the alongshore wind stress. Wind stress curl at the coastal points was then converted to upwelling velocity

(Eq. 6) termed Ekman pumping, whereby W_{Ek} is the Ekman pumping upwelling velocity, ρ_0 is the density of seawater, f is the Coriolis parameter at each latitude and the term in the brackets is wind stress curl. This Ekman pumping velocity results from Ekman divergence within the Ekman layer, as a result of the wind stress curl.

$$W_{Ek} = \frac{1}{\rho_0 f}\left(\frac{\partial \tau_y}{\partial x} - \frac{\partial \tau_x}{\partial y}\right) \quad (6)$$

where wind stress curl = $\frac{\partial \tau_y}{\partial x} - \frac{\partial \tau_x}{\partial y}$

The resultant BUI and Ekman pumping upwelling velocities were then converted to units of metres per day to compare WASA3 and ERA5 January and July climatologies, for all coastal values. While the BUI calculates upwelling velocity over a 20km distance at the coast, Ekman pumping is calculated at the specified coastal points and is therefore not averaged over a specified distance. The total upwelling velocities (the sum of BUI and Ekman pumping upwelling velocities) were also calculated.

3.2.5 Seasonality of upwelling cells

Lastly, upwelling cells were identified from the calculated theoretical upwelling velocities along the coast. Within the study region, the Cape Peninsula, Cape Hangklip and Danger Point upwelling cells were selected. WASA3 was then used to study the seasonality of upwelling in these cells. Theoretical upwelling velocity climatologies were calculated for each month from 1991 to 2019. This was done in the same way as described above (Eq. 1-6), resulting in Ekman pumping upwelling velocity and a BUI upwelling velocity, which were summed to calculate the total upwelling velocity. These were then averaged over the coastal region in each upwelling cell.

4. Results

4.1 Sea surface temperature

Summer (January) and winter (July) climatologies (1991-2019) of SST were plotted for the broader study region (Figure 4.1) to give an overview of the seasonal upwelling dynamics. The study region is shown by the outlined area on Figure 4.1a and b. Upwelling and the resultant uplift of deep water creates regions of cold surface waters, and thus SST is a common method of identifying and studying upwelling regions. While there are inaccuracies associated with satellite SST in upwelling regions (Carr et al., 2021), it is suitable to provide an overview of upwelling dynamics in the study region. The summer climatology shows that SSTs over the broader region tend to be warm especially to the east of the study region due to the presence of the warm Agulhas Current and due to increased solar radiation heating the surface of the ocean during summer (Figure 4.1a). There is a large SST gradient between the warm waters offshore of the west coast of South Africa and the cold waters inshore that extends south to roughly Cape Agulhas, the southern boundary of the WAB and SBUS. The cool inshore SSTs are driven by the intense coastal upwelling that occurs in this region, particularly in summer, the upwelling season in the Southern Benguela. In summer, upwelling can be seen to occur along the entire coast of the Southern Benguela, however it is stronger north of Cape Point, with the coldest SSTs off Cape Columbine indicating the upwelling cell in this region.

Similarly in winter, the Agulhas Current causes warm waters to the east of the WAB, however SSTs over the region are colder due to decreased solar radiation in austral winter (Figure 4.1b). Weaker SST gradients exist between the offshore and coastal waters along the SBUS; however, the offshore waters are still warmer due to the leakage of Agulhas Current water.

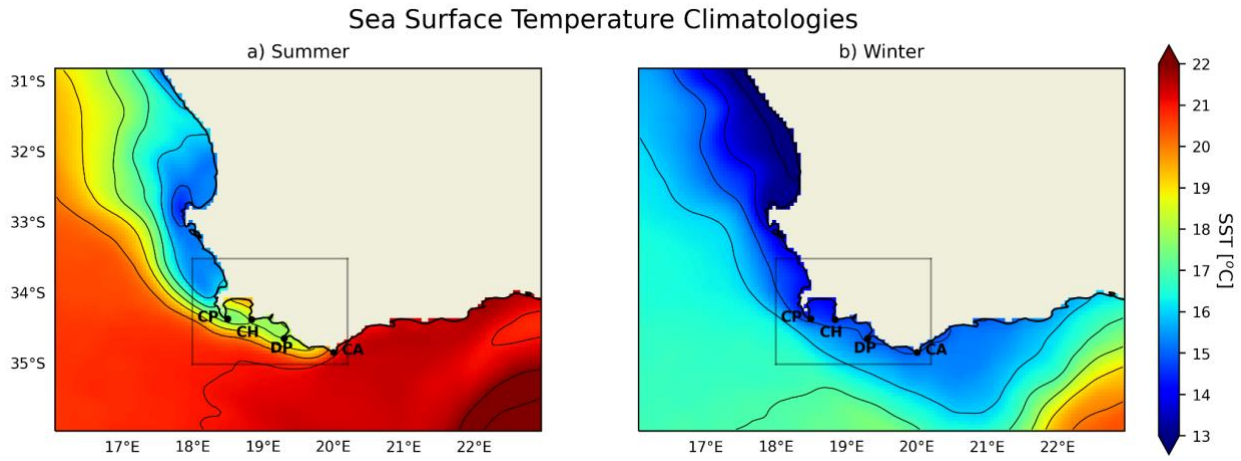

Figure 4.1: Monthly climatology (1991-2019) of OSTIA sea surface temperature (SST) [°C] for a) summer (January) and b) winter (July). Locations of Cape Point (CP), Cape Hangklip (CH), Danger Point (DP) and Cape Agulhas (CA) are shown. Select SST contours are shown in black.

4.2 Wind Stress

Wind stress climatologies for both wind products, ERA5 and WASA3, have been plotted for summer and winter, as wind is the main driver of upwelling (Figure 4.2). Both ERA5 and WASA3 summer wind stress can be seen to be strongly southerly in the region west of South Africa, along the coast of the Southern Benguela, with stronger easterly components offshore of the WAB, parallel to the coastline. Wind stress is stronger along the west coast from Cape Hangklip northwards, with weaker, more onshore winds to the east of Cape Hangklip.

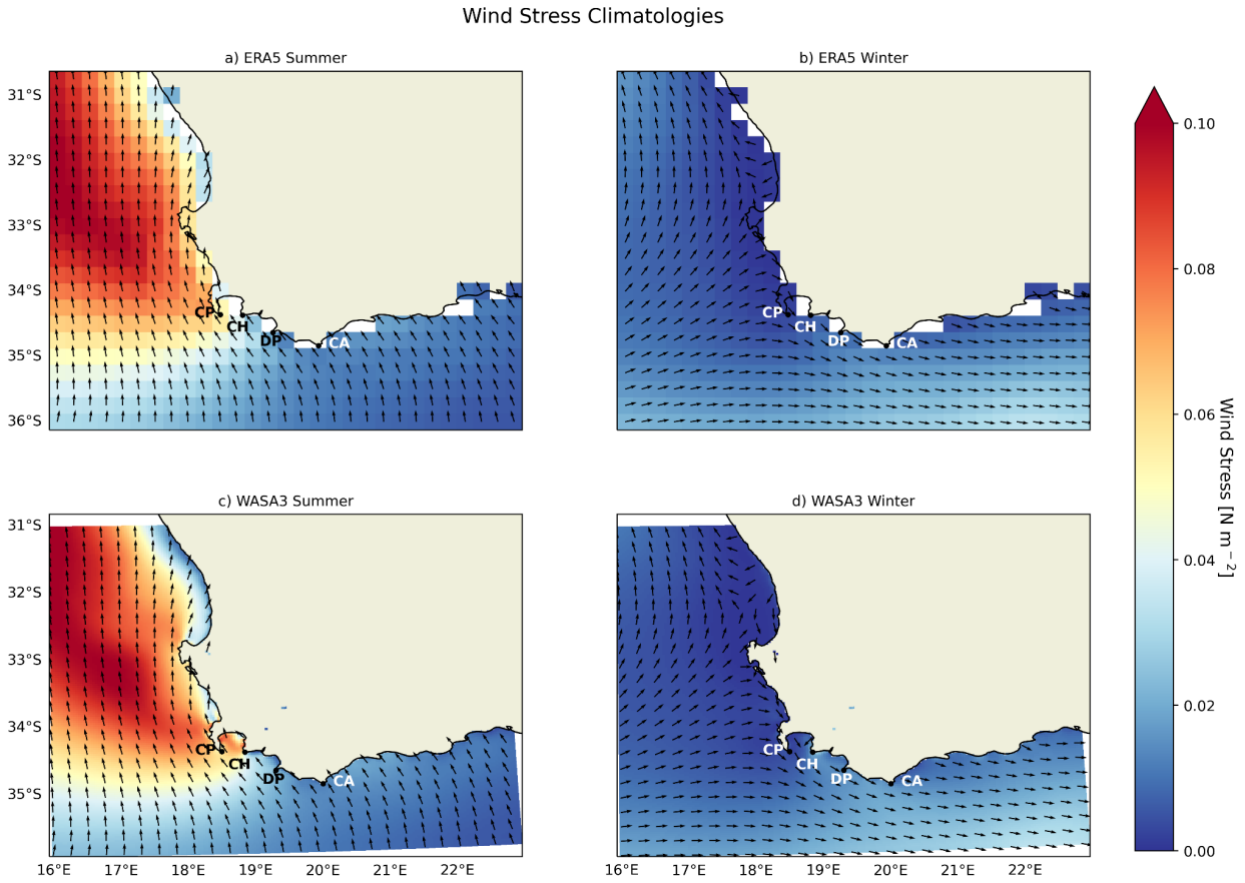

Figure 4.2: ERA5 and WASA3 wind stress [N m^{-2}] climatologies (1991-2019) for a, c) summer (January) and b, d) winter (July). Normalised wind stress quivers have been plotted for every grid point in the ERA5 dataset, and every 7th grid point in the WASA3 dataset. Locations of Cape Point (CP), Cape Hangklip (CH), Danger Point (DP) and Cape Agulhas (CA) are shown.

The winter wind stress climatologies show weak wind stress on average with westerly directions south of South Africa and slightly southerly directions west of South Africa in both ERA5 and WASA3. This is indicative of highly variable wind directions in winter which when averaged, result in low wind stress magnitudes. Over the WAB, wind stress is weak with a north-westerly direction along the coast on average, in the opposite direction to summer.

The magnitude and direction of wind stress for both ERA5 and WASA3 in both summer and winter compared well on a broad scale. However, it is evident that ERA5 is not able to resolve the bay-scale features due to its lower spatial resolution. This is evident over False Bay, where ERA5 provides incomplete coverage, and WASA3 is able to capture differences in wind stress within the bay, and a wind drop off in the wind shadow of the Cape Hangklip mountains in summer (Figure 4.2c). WASA3 also shows a wind drop off near the coast in Table Bay, north

of the Cape Peninsula, in summer that ERA5 does not capture. Wind drop offs can also be seen along other coastal regions in the WAB in the WASA3 derived wind stress, such as near the coast between Cape Hangklip and Danger Point in summer (Figure 4.2c), as well as west of Cape Hangklip in winter (Figure 4.2d). These variations captured in WASA3 have the potential to largely impact upwelling along the coast.

4.3 Wind stress curl

Wind stress curl for both wind products has been plotted for the broader region for summer and winter climatologies (Figure 4.3). Negative wind stress curl (blue) indicates the clockwise, cyclonic rotation of the wind field which, in the Southern Hemisphere, results in Ekman divergence within the Ekman layer and 'Ekman suction', i.e., upwelling. Conversely, positive wind stress curl (red) indicates anticlockwise rotation of the wind field in the Southern Hemisphere, resulting in 'Ekman pumping', i.e., downwelling.

In summer, strong negative wind stress curl can be seen along the west coast in both ERA5 and WASA3 climatologies (Figure 4.3a, c). While WASA3 shows stronger negative wind stress curl over the parts of the oceanic region off the west coast, the strongest differences between the two wind products occur at the coast in the SBUS (Figure 4.3e). The higher resolution of WASA3 shows a much clearer representation of small-scale variations at the coast such as in False Bay where the bay is divided into a region of strongly negative wind stress curl on the northeast side, and positive wind stress curl on the southwestern side. There is also much more variation in wind stress curl along the coast of the Southern Benguela, north of Cape Hangklip, with regions of strongly negative wind stress curl on the west of the Cape Peninsula, north of Cape Columbine and on the north-eastern side of False Bay (Figure 4.3c). This is consistent with the fact that it reproduces a much stronger wind shadow and drop off in wind stress towards the coast in these regions (Figure 4.2c). ERA5 is unable to capture the wind stress curl and variations at a fine scale along the coast due to its coarse resolution, clearly seen in the summer wind stress curl (Figure 4.3a).

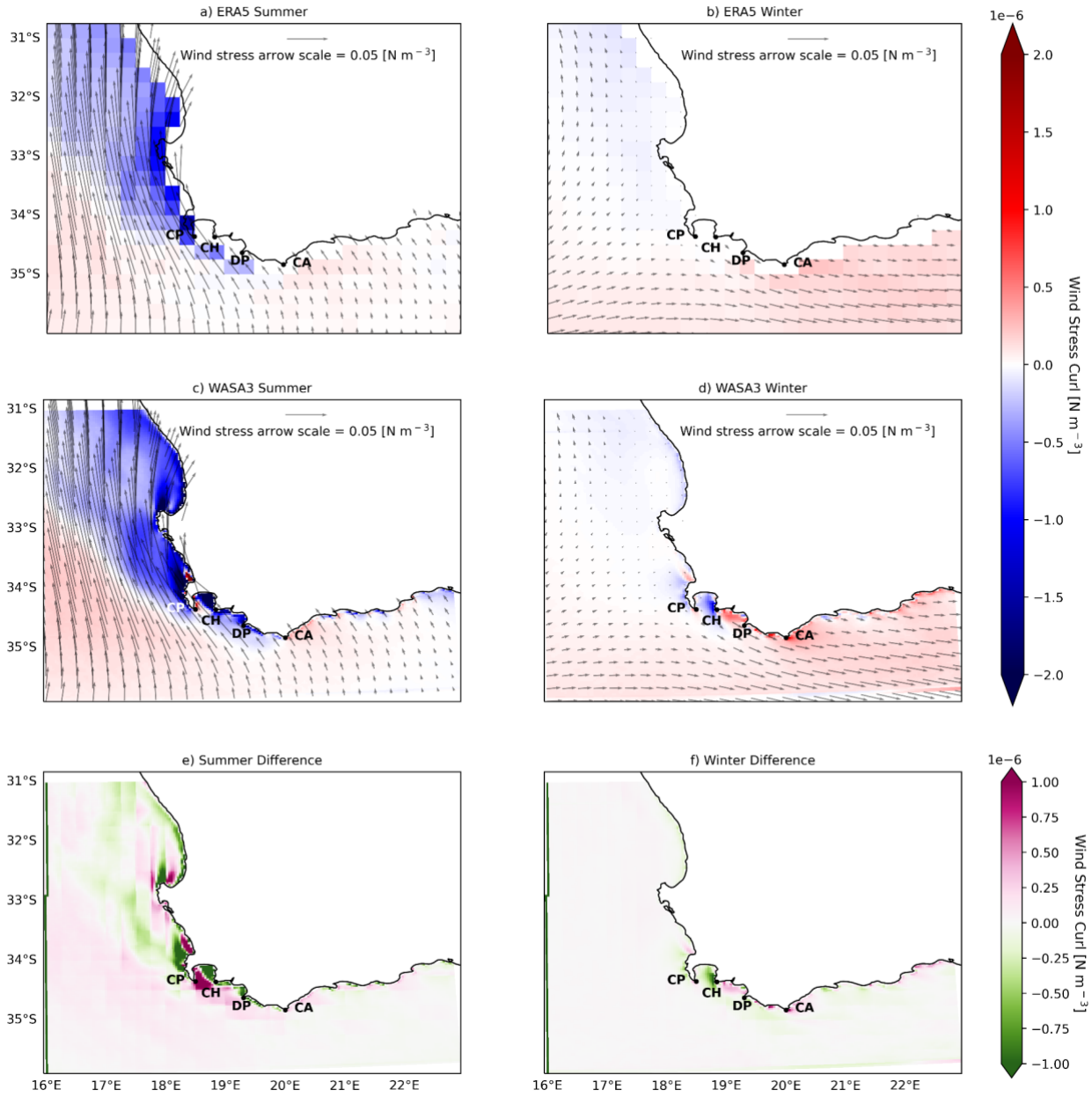

Figure 4.3: ERA5 and WASA3 wind stress curl [N m^{-3}] climatologies for a, c) summer (January) and b, d) winter (July) for 1991 to 2019, and the difference between WASA3 and ERA5 wind stress curl climatologies for e) summer and f) winter. The difference between wind products has been calculated using an interpolated ERA5 dataset. Wind stress quivers have been plotted for every grid point in the ERA5 dataset, and every 7th grid point in the WASA3 dataset. Locations of Cape Point (CP), Cape Hangklip (CH), Danger Point (DP) and Cape Agulhas (CA) are shown.

In winter, there is little variation in the wind stress curl across the entire region in ERA5 with weakly negative values off the west coast, and weakly positive values south of South Africa

(Figure 4.3b). In WASA3 the offshore wind stress curl is very similar in winter, however there is stronger negative wind stress west of the Cape Peninsula and Cape Hangklip, and weakly along the coast north of Cape Columbine, with stronger positive wind stress curl concentrated east of Cape Hangklip and extending along the coast to the east (Figure 4.3d, f). WASA3 captures these stronger coastal values due to its ability to reproduce the wind drop off along the coast, and wind shadows downwind of capes.

4.4 Alongshore wind stress over the WAB

Alongshore wind stress controls the amount of offshore Ekman transport and thus the BUI. In the Southern Hemisphere, transport occurs to the left of the wind, and thus in this study positive alongshore wind corresponds to upwelling favourable wind. The summer climatological values of alongshore wind stress along the coastline (see Data and Methods for identification of these values) for ERA5 and WASA3 show predominantly positive alongshore wind stress, with strongly positive alongshore wind stress along the west of the Cape Peninsula (Figure 4.4a, c). Both ERA5 and WASA3 also show strongly negative alongshore wind stress on the west side of False Bay, however, WASA3 has stronger negative values in this region (Figure 4.4e). WASA3 has weaker upwelling favourable winds north of Cape Point, consistent with the enhanced wind drop off seen in WASA3 along the coast in this region (Figure 4.2c). Figure 4.4e also shows a large difference in alongshore wind stress on the east of False Bay at Cape Hangklip, where WASA3 shows much stronger, positive values of wind stress in this region (Figure 4.4a, c, e).

The standard deviation of ERA5 and WASA3 has been plotted as a measure of intraseasonal and interannual variability. The standard deviations of both wind products show increases along the coast to the west, with higher values of standard deviation in wind around False Bay and the Cape Peninsula than the regions to the east (Figure 4.4b, d), showing that winds to the east are less variable in summer. The difference between WASA3 and ERA5 standard deviation shows that WASA3 winds have a higher standard deviation around the majority of the coast, particularly Cape Hangklip and Table Bay, two regions where WASA3 captures stronger negative wind stress curl associated with the wind shadow in these regions (Figure

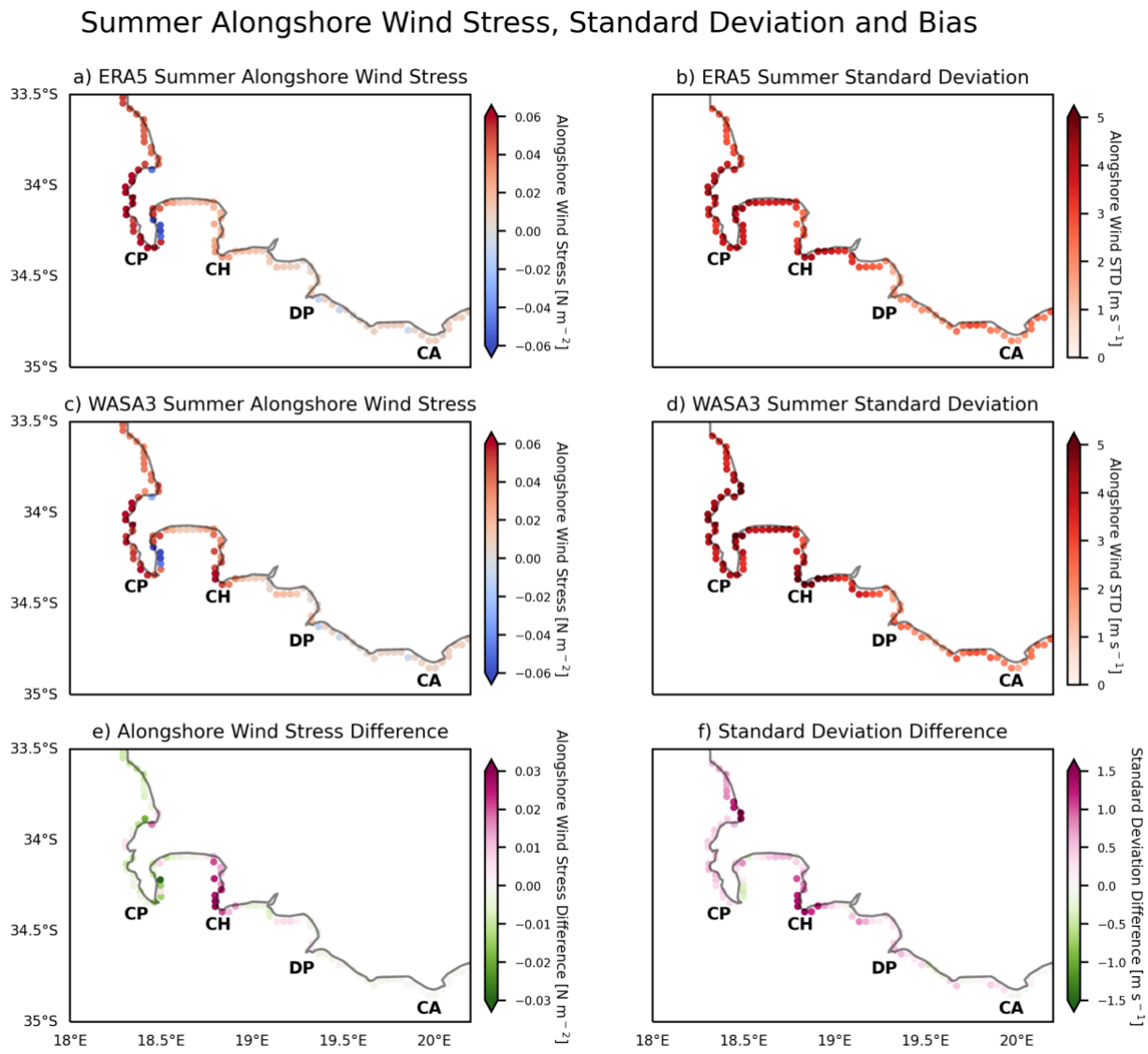

Figure 4.4: Summer (January) a) ERA5 and c) WASA3 alongshore wind stress [N m^{-2}] climatologies (1991-2019) and e) the difference between WASA3 and ERA5 January coastal wind stress for the WAB and surrounds. Positive (negative) values refer to upwelling (downwelling) favourable wind stress. The standard deviations of January alongshore wind are plotted for b) ERA5 and d) WASA3 as well as f) the difference between WASA3 and ERA5 standard deviations. Locations of Cape Point (CP), Cape Hangklip (CH), Danger Point (DP) and Cape Agulhas (CA) are shown.

4.4f). This indicates that despite the two products having the same temporal resolution, WASA3 reproduces more temporal variability in the wind field due to its higher spatial resolution.

The coastal values of alongshore wind stress for winter for ERA5 and WASA3 show weakly negative values of alongshore wind stress with stronger negative values in Walker Bay, between Cape Hangklip and Danger Point, in WASA3 (Figure 4.5a, c, e). The standard deviation of ERA5 and WASA3 shows that both wind products have high standard deviations along the coastline in winter, increasing towards the west, indicating highly variable winds.

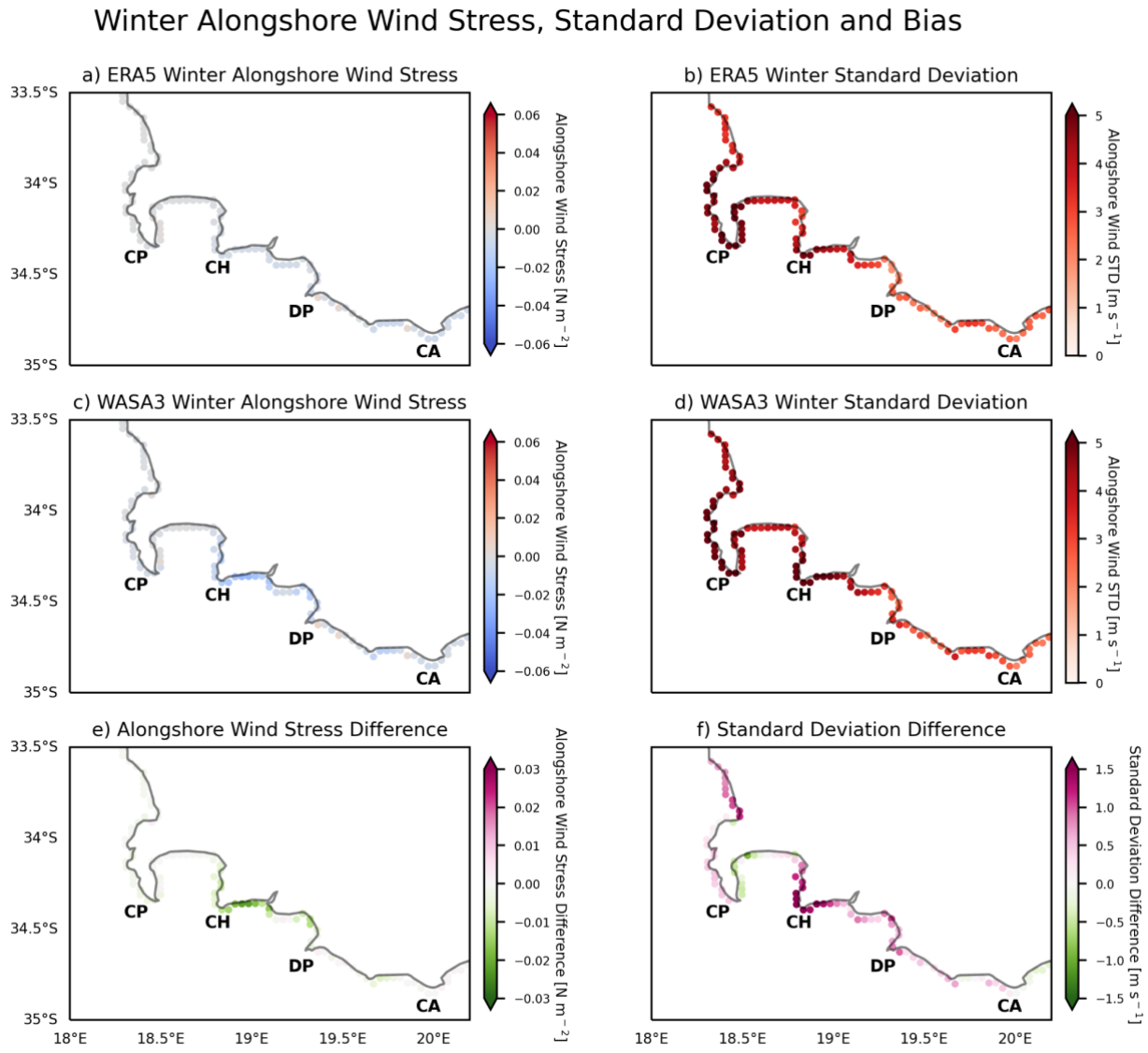

Figure 4.5: Winter (July) a) ERA5 and c) WASA3 coastal wind stress [N m^{-2}] climatologies and e) the difference between WASA3 and ERA5 July alongshore wind stress for the WAB and surrounds. Positive (negative) values of alongshore wind stress refer to upwelling (downwelling) favourable wind stress. The standard deviations of alongshore wind are plotted for b) ERA5 and d) WASA3 July values from 1991 to 2019, as well as f) the difference between WASA3 and ERA5 standard deviations. Locations of Cape Point (CP), Cape Hangklip (CH), Danger Point (DP) and Cape Agulhas (CA) are shown.

The winter standard deviations are higher than the summer standard deviations for both wind products, showing larger variability in wind in winter (Figure 4.4a, c; Figure 4.5a, c). The difference in WASA3 and ERA5 standard deviations for winter show that, as seen in summer, WASA3 has more variable winds in Table Bay, west of the Cape Peninsula, around Cape Hangklip and extending down to Cape Agulhas due to its ability to capture small scale features such as wind shadows and drop offs. Conversely, ERA5 has a higher variability in wind on the western side of False Bay (Figure 4.5e).

4.5 Wind stress curl over the WAB

Wind stress curl induces Ekman pumping, and acts to either suppress or enhance upwelling. In the Southern Hemisphere, negative wind stress curl causes positive Ekman pumping and enhances upwelling. Wind stress curl, in conjunction with alongshore wind (Figure 4.5), are the two controls on resultant wind-driven upwelling, and are thus studied on the WAB to understand upwelling dynamics. The ERA5 summer wind stress curl shows negative values throughout the coast of the WAB, with the strongest negative wind stress curl north of the WAB in Table Bay (Figure 4.6a). WASA3 also shows negative wind stress curl along much of the coast in this region, however there are also regions of positive wind stress curl in WASA3 that are not captured in ERA5, such as in Table Bay and the western side of False Bay (Figure 4.6c). There is much more variation in the values of wind stress curl along the coast in WASA3 compared to ERA5, with stronger negative wind stress curl in WASA3 in the eastern side of False Bay and the western side of the Cape Peninsula, due to the higher resolution of the dataset being able to resolve the topographical effects of the headlands and the wind shadows they create.

In winter, ERA5 shows weakly positive wind stress curl over the majority of the region (Figure 4.6b), whereas WASA3 shows negative wind stress curl on the east of False Bay and the west of the Cape Peninsula due to its ability to capture a wind drop off. WASA3 also shows positive wind stress curl of a greater magnitude in Walker Bay and along the coast to the east (Figure 4.6d). While in summer, the upwelling season, there is predominantly strong, negative wind stress curl along the coast in this region, in winter, there is mostly positive wind stress curl

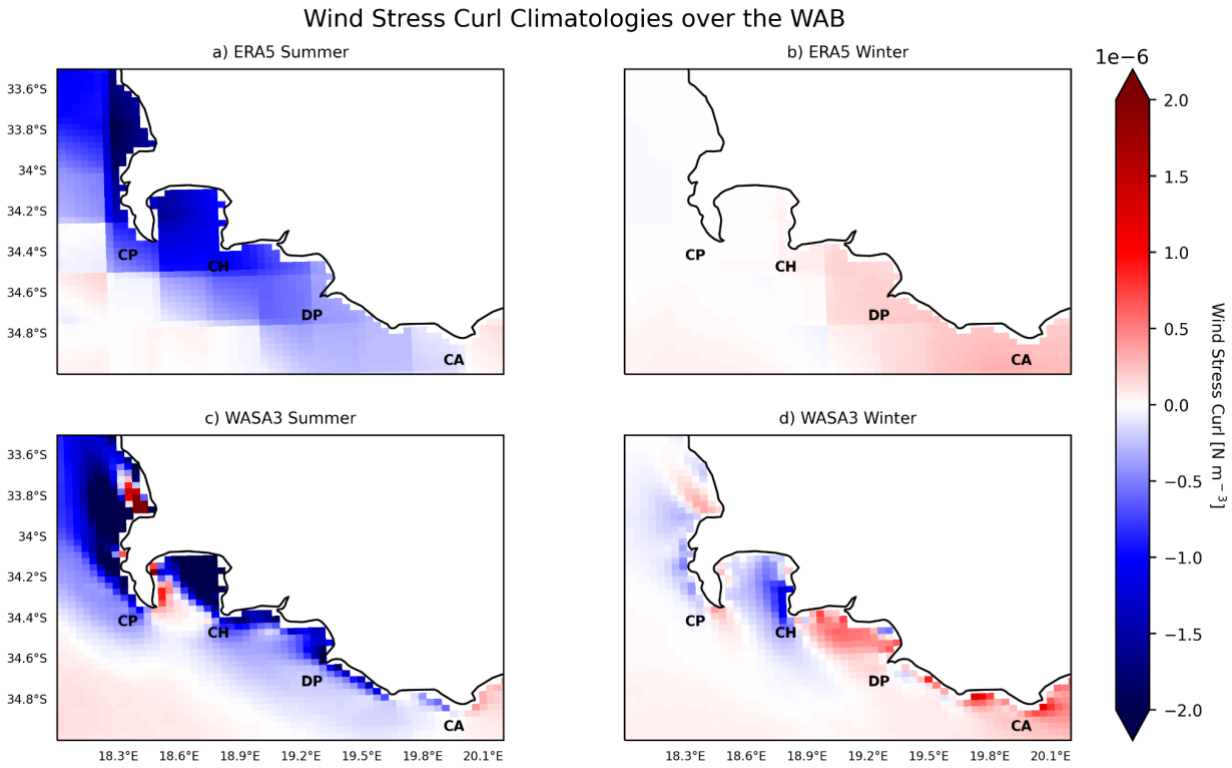

Figure 4.6: ERA5 and WASA3 wind stress curl [N m^{-3}] climatologies over the WAB for a, c) January and b, d) July for 1991 to 2019. ERA5 has been interpolated bilinearly to the same grid as WASA3. Locations of Cape Point (CP), Cape Hangklip (CH), Danger Point (DP) and Cape Agulhas (CA) are shown.

which would suppress upwelling, except on the eastern side of False Bay and the western side of the Cape Peninsula. This shows that orography-induced wind stress curl may enhance upwelling in this region, even in winter.

4.6 Upwelling Velocities

The derived theoretical upwelling velocities plotted below (Figure 4.7) show that both wind products generally show larger values of positive upwelling velocities in summer than in winter, however the total upwelling velocities, relative contribution of BUI and EP, and area where the upwelling is concentrated along the coast differ largely between ERA5 and WASA3 in both seasons.

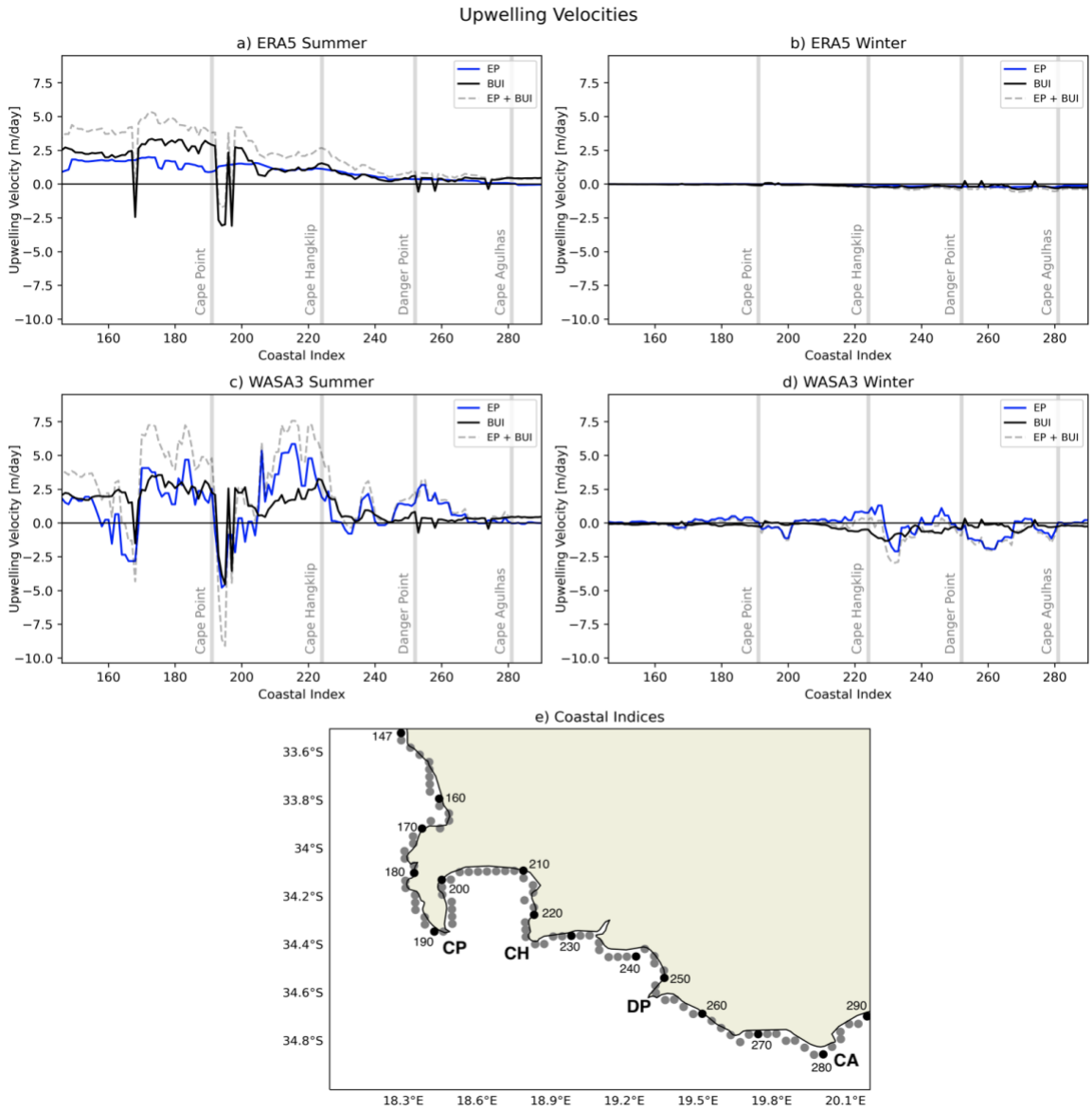

Figure 4.7: ERA5 and WASA3 theoretical upwelling velocities [m day^{-1}] along the coast of the WAB for a, c) the January climatology and b, d) the July climatology. Positive (negative) upwelling velocities represent upwelling (downwelling). The blue line represents Ekman pumping (EP) upwelling velocity, which results from wind stress curl. The black line represents the BUI upwelling velocity as a result of offshore Ekman transport. The grey, dashed line represents the total upwelling velocity. The grey, vertical lines represent the coastal index of the Capes along the WAB. Left (right) on the x-axis points along the coastline to the west (east). The location of coastal indices, Cape Point (CP), Cape Hangklip (CH), Danger Point (DP) and Cape Agulhas (CA) are shown, e).

In summer, both ERA5 and WASA3 show positive upwelling velocities west of Cape Point, however WASA3 shows a larger magnitude and a higher contribution of EP than ERA5. This is consistent with the results above that show that WASA3 captures more spatial variability and

stronger negative wind stress curl at capes, which enhances upwelling in these regions (Figure 4.3, 4.7a, 4.7c).

East of Cape Point, both products show downwelling in the region on the west side of False Bay, however again the magnitude of WASA3 and the contribution of wind stress curl in WASA3 are greater. In ERA5, Ekman pumping is positive in this region, indicating that it theoretically reduces the downwelling captured by ERA5, whereas in WASA3, Ekman pumping is negative, enhancing the downwelling represented in this dataset. West of Cape Hangklip in the region on the eastern side of False Bay, WASA3 shows larger values of upwelling, and again a larger contribution of Ekman pumping to the total upwelling velocity than in ERA5. This shows WASA3's ability to capture more spatial variability, particularly in the wind stress curl that drives Ekman pumping, such as the large difference across False Bay that is not captured in ERA5 (Figure 4.7a, c).

ERA5 shows little upwelling around Danger Point and Cape Agulhas in summer, however WASA3 captures some upwelling occurring around Danger Point, predominantly driven by EP and thus wind stress curl. The summer plots also show that the BUI tends to be similar in magnitude and area between ERA5 and WASA3, however the EP differs largely in magnitude and area on the coast, which drives the differences observed between the two products (Figure 4.7a, c).

In winter, there is a larger difference between WASA3 and ERA5 especially eastward of Cape Point. ERA5 shows very small values of upwelling or downwelling along the coast, however WASA3 captures patterns in upwelling and downwelling driven primarily by Ekman pumping, especially in the regions further east along the WAB (Figure 4.7b, d). WASA3 captures primarily downwelling along the WAB, between Cape Point and Cape Agulhas. While the total upwelling velocity around Cape Hangklip is near zero, the negative wind stress curl observed above in winter (Figure 4.6) can be seen to cause some positive EP, but downwelling as a result of BUI opposes this. East of Cape Hangklip, there is downwelling captured, caused by both wind stress curl and negative offshore Ekman transport. East of Danger Point, there is a region of downwelling resulting from wind stress curl, with some downwelling also occurring

west of Cape Agulhas. In winter, the total upwelling derived from WASA3 is predominantly controlled by the EP velocity, as a result of wind stress curl (Figure 4.7d).

4.7 Seasonality of upwelling cells

Three coastal regions of strong theoretical wind-driven upwelling velocities are evident in the WASA3 summer upwelling velocities (Figure 4.7c). The region west of Cape Point, with a coastal index of 170 to 191 (Figure 4.7c), shows strong positive upwelling velocities in summer. This coastal region corresponds to the Cape Peninsula (CP) upwelling cell, which has been well defined in the literature (Lutjeharms and Meeuwis, 1987; Nelson et al., 1998). The coastal region west of Cape Hangklip (CH), with a coastal index of 213 to 224 (Figure 4.7c) shows a total upwelling velocity of a similar magnitude to that found in the Cape Peninsula upwelling cell. There is upwelling evident at the coast around Danger Point (DP), with a coastal index of 248 to 259 (Figure 4.7c). WASA3 was used to study these three regions of upwelling as the results shown above demonstrate that ERA5 does not capture distinct regions of upwelling (Figure 4.7a, c).

WASA3-derived wind-driven upwelling velocities over the Cape Peninsula upwelling cell show that the maximum BUI, Ekman pumping and total upwelling occurs in January, where Ekman pumping (50.38%) and BUI (49.62%) contribute almost equally to total upwelling (Figure 4.8; Table 4.1). There is a clear seasonal cycle with larger upwelling values in summer months, as expected as summer is the upwelling season in this region. Of the total upwelling during each month, Ekman pumping upwelling induced from wind stress curl contributes similarly to BUI from alongshore wind, however during winter months, the positive upwelling Ekman pumping upwelling velocities oppose the negative BUI upwelling velocities, resulting in a total upwelling velocity of around zero. BUI and Ekman pumping also have similar standard deviations, indicating a similar seasonal variability.

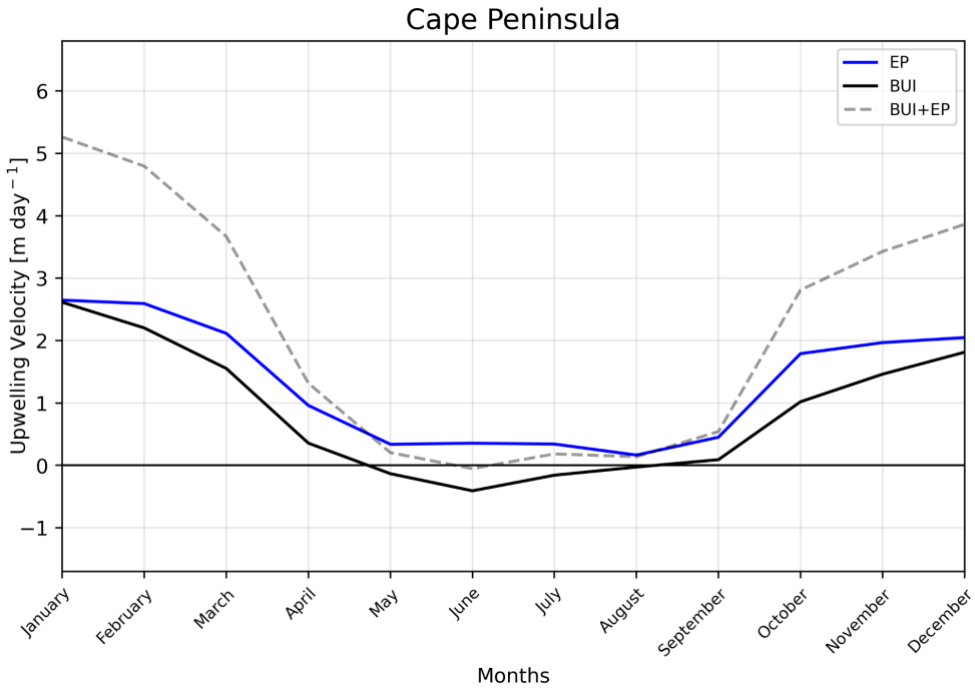

Figure 4.8: WASA3 theoretical Ekman pumping (EP, blue) upwelling velocity, Bakun Upwelling Index (BUI, black) and total upwelling velocity (EP + BUI, black dashed) [m day^{-1}] in the Cape Peninsula upwelling cell for each month from 1991 to 2019.

Unlike at the Cape Peninsula upwelling cell, at Cape Hangklip Ekman pumping (67.23%) contributed just more than double the contribution of BUI (32.77%) to the total upwelling velocity in January, the month of maximum upwelling (Table 4.1). The percentage contribution of Ekman pumping to total upwelling reduces during winter months, however the positive Ekman pumping velocities oppose the negative BUI velocities resulting in total upwelling near to zero, except in June where there is downwelling evident. In winter months, similarly to Cape Peninsula, the magnitudes of Ekman pumping upwelling velocities are low, indicating less wind stress curl likely due to weaker winds in the climatology and thus a weaker wind drop off at the coast (Figure 4.2). The seasonal cycle of wind-driven upwelling is similar to that off the Cape Peninsula, with stronger upwelling in summer months, and the maximum of all upwelling metrics in January (Table 4.1, Figure 4.9). Ekman pumping has a higher standard deviation than BUI indicating larger seasonal variability, unlike in the Cape Peninsula cell. The Cape Hangklip cell shows higher variability in Ekman pumping and total upwelling velocities, indicating it has higher seasonal variability than the two other cells.

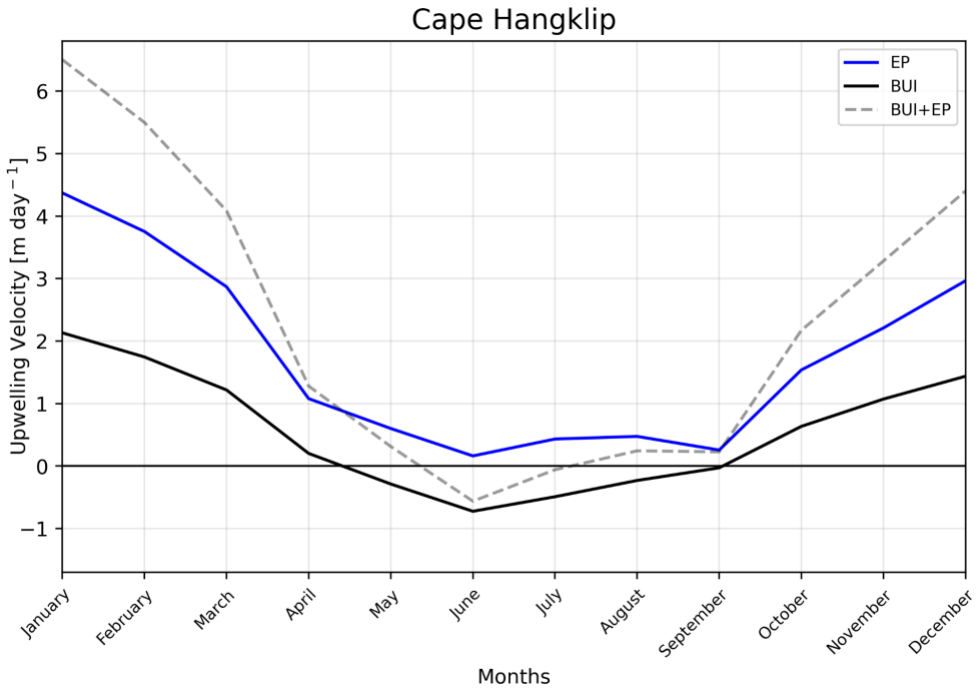

Figure 4.9: WASA3 theoretical Ekman pumping (EP, blue) upwelling velocity, Bakun Upwelling Index (BUI, black) and total upwelling velocity (EP + BUI, black dashed) [m day^{-1}] at Cape Hangklip for each month from 1991 to 2019.

While the upwelling at Cape Peninsula and Cape Hangklip showed similar values of upwelling and seasonal cycles, upwelling at Danger Point differs in that Ekman pumping is the dominant contributor to total wind-driven upwelling velocities, contributing 87.85% in January, the month of maximum upwelling (Table 4.1). BUI has a low contribution in all months, with a low seasonal standard deviation indicating low variability throughout the year, compared to Ekman pumping with a higher standard deviation (Figure 4.10; Table 4.1). While Danger Point shows a similar seasonal cycle, there are lower values of total upwelling at Danger Point throughout the year, with notable negative upwelling velocities in winter months, indicating stronger downwelling than in the other two regions (Figure 4.10).

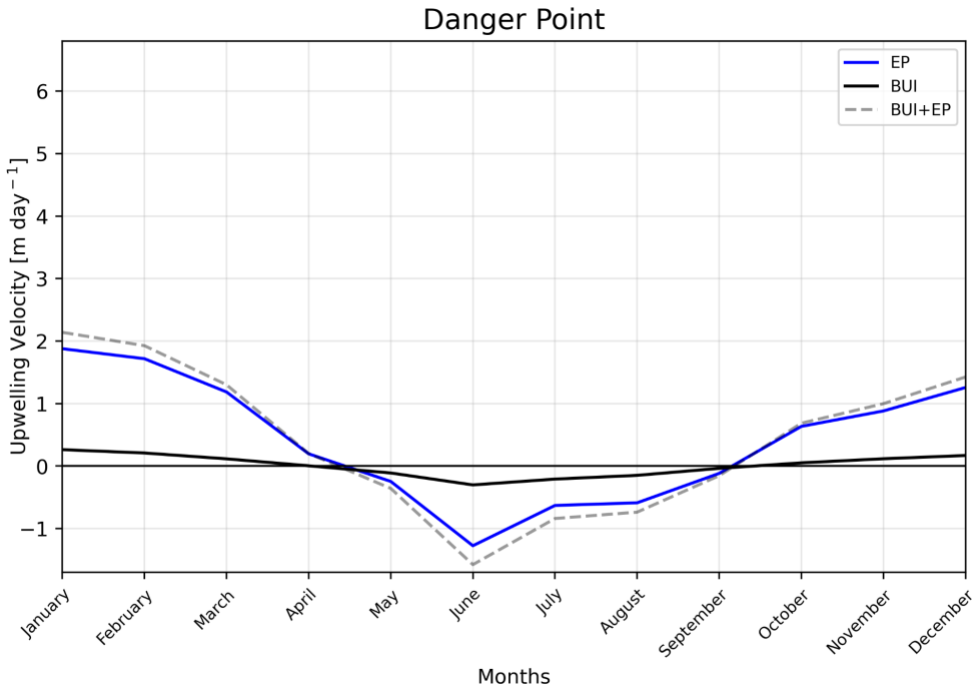

Figure 4.10: WASA3 theoretical Ekman pumping (EP, blue) upwelling velocity, Bakun Upwelling Index (BUI, black) and total upwelling velocity (EP + BUI, black dashed) [m day^{-1}] at Danger Point for each month from 1991 to 2019.

Table 4.1: WASA3 maximum and minimum Bakun Upwelling Index (BUI), Ekman pumping (EP) and total upwelling velocities [m day^{-1}], the month they occur in and the seasonal standard deviation (SD) of each upwelling metric at Cape Peninsula (CP), Cape Hangklip (CH) and Danger Point (DP).

Region	Upwelling metric	Max upwelling velocity [m day^{-1}]	Month	Min upwelling velocity [m day^{-1}]	Month	Seasonal SD [m day^{-1}]
CP	BUI	2.61	January	-0.41	June	1.04
	EP	2.65	January	0.16	August	0.97
	Total	5.26	January	-0.05	June	2.00
CH	BUI	2.13	January	-0.72	June	0.95
	EP	4.37	January	0.16	June	1.47
	Total	6.50	January	-0.56	June	2.41
DP	BUI	0.26	January	-0.30	June	0.18
	EP	1.88	January	-1.28	June	1.01
	Total	2.14	January	-1.58	June	1.18

5. Discussion

The results presented in this thesis investigate seasonal upwelling on the WAB, based on theoretical, wind-driven upwelling metrics derived from the output of two atmospheric models: a low- and high-resolution wind product. This has been done to determine the extent to which a higher resolution wind product might impact wind-driven upwelling velocities in numerical ocean models and to identify and describe the seasonal cycle of regions of upwelling in the understudied WAB.

5.1 ERA5 vs WASA3

ERA5 and WASA3 were both used to calculate key variables in the study of upwelling, namely wind stress, wind stress curl, alongshore wind stress and the derived theoretical wind-driven upwelling velocities along the South African coast. This allowed for the effects of WASA3's higher spatial resolution to be determined on upwelling studies in the region, given that the temporal resolution and time span was kept constant in both wind products.

While similarities between the two wind products were found for the large-scale offshore region, there were inconsistencies closer to the coast. Wind stress showed inconsistencies in False Bay and along the coast of the Southern Benguela, where the coarse resolution of ERA5 is unable to capture small scale features such as the wind drop off along the coast and wind shadows downwind of headlands. This results in large differences in wind stress curl between the two products, particularly along the coast of the SBUS in summer, the main upwelling season (Figure 4.3e). Negative wind stress curl induces upwelling in the Southern Hemisphere, and it determines the location of upwelling cells in the SBUS. Changes in orientation of the coastline induce negative wind stress curl downwind of prominent headlands and form upwelling cells (see page 6), such as Cape Columbine and Cape Point (Bentamy et al., 2021; Jury, 2020; Nelson, 1981). WASA3 captures stronger negative wind stress curl at Cape Point and Cape Hangklip in summer, the upwelling season, with stronger positive wind stress curl at the coast in Table Bay and on the western side of False Bay, where downwelling occurs. This is due to WASA3's ability to capture wind drop offs at the coast and wind shadows which induce wind stress curl, as can be seen by the weaker coastal wind stress particularly along

the west coast (Figure 4.2c). Orography-induced wind stress curl occurs at fine spatial scales, and thus a higher resolution wind dataset, such as WASA3, is able to capture these small-scale processes (Desbiolles et al., 2014), as shown by the large differences in wind stress curl compared to ERA5 (Figure 4.3e).

Wind stress curl drives Ekman pumping and locations of upwelling cells (Bentamy et al., 2021), and thus ERA5's inability to capture small scale variations in wind stress curl translates into ERA5 not resolving Ekman pumping's contribution to total upwelling velocities. Conversely, the WASA3 wind-driven upwelling velocities identify clear regions of higher upwelling rates, such as west of Cape Point and Cape Hangklip, at changes in orientation of the coastline and prominent headlands that induce wind stress curl (Figure 4.7). While both products show higher upwelling rates in summer, in agreement with this being the main upwelling season in the region (Shannon and Nelson, 1996), WASA3 shows greater magnitudes of upwelling off Cape Point, Cape Hangklip and Danger Point due to the increased contribution of wind stress curl induced upwelling in those regions. In winter, WASA3 also shows greater magnitudes of upwelling and downwelling predominantly driven by wind stress curl driven Ekman pumping, compared to ERA5 which represents almost no vertical velocity along the coast. BUI is more similarly represented in both products in both seasons, indicating that the large differences in total upwelling velocities are mainly driven by the differences in Ekman pumping across wind products and WASA3's ability to capture small-scale orography induced wind stress curl.

ERA5 is commonly used to force numerical ocean models used around South Africa, for example recent GLORYS12V1 (here on out referred to as GLORYS) reanalysis runs from 2019 onwards, which were previously forced with ERA-Interim (DOI: https://doi.org/10.48670/moi-00021). Generally, ERA5 has been reported to have accurate representations of winds (Olauson, 2018), however it has been shown that the wind values at the coast over Eastern Boundary Currents, such as the Benguela and the associated upwelling region, are unrealistic (Strub and James, 2022). This is likely due to an inability of ERA5 to capture the wind drop off near the coast due to its low spatial resolution of 31 km, as shown in this thesis. This wind drop off is essential in accurately modelling upwelling velocities as it induces wind stress curl and resultant vertical velocities that either enhance or

suppress upwelling and determine the location of upwelling cells (Bentamy et al., 2021; Shannon and Nelson, 1996).

Models forced with ERA5, or wind products of equivalent coarse resolutions (>30km) are notoriously bad at resolving upwelling structures and resultant SSTs in EBUSs (Russo et al., 2022). This inability to correctly resolve upwelling structures can lead to a warm bias which is common in global and regional model representations of SSTs along the coast in EBUSs (Ragoasha et al., 2019; Russo et al., 2022; Small et al., 2015). The largest warm bias out of all the EBUSs in global climate models is seen in the Benguela Upwelling System (Small et al., 2015). In addition, GLORYS shows a persistent warm bias throughout the water column in the SBUS in the upwelling season. Coarse wind products used in global and regional models poorly resolve coastal winds in EBUSs (Richter, 2015), and use of a higher resolution wind product will likely improve their accuracy in modelling upwelling structures.

This thesis highlights that models using low resolution winds won't capture upwelling centres along the WAB, especially those driven by wind stress curl. The results shown in this thesis, in conjunction with previous literature, thus recommend caution when interpreting upwelling related variables simulated in models using ERA5 or wind products of comparable resolution. The importance of wind stress curl and small-scale processes in upwelling demonstrated in this thesis point towards a need for regional and global climate models to use higher resolution wind forcing, such as WASA3, to allow them to improve simulations of EBUSs and determine the effects of a spatially varying wind field on upwelling (Coleman, 2019; Desbiolles et al., 2014). This is particularly necessary in the WAB, as upwelling in this region is understudied, and this thesis has shown that wind stress curl is the dominant forcing mechanism of wind-driven upwelling in parts of the WAB, indicating that understanding of upwelling in this region would benefit from improved model simulations.

5.2 Upwelling Dynamics on the WAB

Upwelling in the WAB, from Cape Point to Cape Agulhas, is understudied compared to the rest of the SBUS, such as the Cape Peninsula upwelling cell, which has been included in the study region of this thesis for comparison to the WAB. Previous work on the WAB has shown

upwelling to occur west of Cape Hangklip (Coleman et al., 2021; Cram, 1970; Jury, 1984), Danger Point (Boyd et al., 1985; Dufois and Roualt, 2012; Jury, 1988; Largier et al., 1992) and Cape Agulhas (Dufois and Roualt, 2012; Largier et al., 1992). The results presented in this thesis show that based on the high resolution WASA3 wind product, strong upwelling is expected west of Cape Point at the Cape Peninsula upwelling cell; west of Cape Hangklip and along the coast surrounding Danger Point in summer in agreement with the literature. The results however show no indication of wind-driven upwelling at Cape Agulhas in the summer climatology (Figure 4.7c), despite this region being defined as one of the upwelling cells of the SBUS (Dufois and Roualt, 2012; Largier et al., 1992; Lutjeharms and Meeuwis, 1987). Upwelling favourable winds off Cape Agulhas have a strong easterly component and are less frequent during summer which has been described as causing irregular, periodic upwelling (Jury, 1988), in agreement with the results in this thesis showing average summer winds to have stronger southerly, onshore components around Cape Agulhas (Figure 4.2c). Future work should study maximum forcing scenarios to identify whether this upwelling is intermittent, driven by periods of winds with strong easterly components, and is thus the reason it is not being seen in the climatology. The methods used in this study are based on theoretical wind-driven upwelling, however there are other factors that influence upwelling along the coast. Specifically interactions between coastal upwelling and the Agulhas Current may result in additional current driven upwelling and stratification feedback both of which are not well understood in this region. Future work should therefore also identify whether there are other processes that may be enhancing upwelling at Cape Agulhas that have not been included in this study.

The results in this thesis show strong upwelling west of Cape Hangklip in summer, in agreement with *in situ* oceanographic surveys, model output and in SST satellite imagery that found upwelling in this region (Coleman et al., 2021; Cram, 1970; Dufois and Roualt, 2012). Upwelling west of Cape Hangklip has been attributed to the south easterly winds in summer inducing negative wind stress curl as they are orographically channelled around the prominent headland of Cape Hangklip, as seen to be well represented by the WASA3 dataset (Figure 4.6c; Jury, 2020; Largier, 2020; Nelson, 1981; Wainman et al., 1987).

The total upwelling velocity of west of Cape Hangklip represented by WASA3 is larger in magnitude to that of the Cape Peninsula upwelling cell in January, the month of maximum upwelling (Figure 4.7c; Table 4.1), however stronger upwelling at Cape Hangklip than at the Cape Peninsula cell is not seen *in situ*. The results presented in this thesis suggest stronger upwelling velocities at Cape Hangklip based on wind-driven upwelling alone, however the stronger upwelling at the Cape Peninsula cell seen *in situ* is likely due to other factors that are not included in this study. This study used only theoretical wind-driven upwelling metrics and did not take into account other factors that affect upwelling. The Cape Peninsula upwelling cell is a well-studied cell (Lutjeharms and Meeuwis, 1987), and according to the literature has a faster response to upwelling favourable winds than the WAB to the east of Cape Point (Boyd et al., 1985). This has been attributed to other processes off the Cape Peninsula that facilitate the uplift of water to the surface faster than on the WAB, such as increased availability of source water, steep bathymetry, the presence of submarine canyons that channel water to the surface and less stratification (Abrahams et al., 2021; Boyd et al., 1985; Chapman and Largier, 1989; Nelson, 1981). Therefore, given these results of similar values of upwelling velocities, it is likely that in reality the other factors not accounted for in this study explain a stronger upwelling cell off Cape Peninsula than off Cape Hangklip seen *in situ*.

A similar mechanism causing upwelling off Cape Hangklip has been suggested to exist off Danger Point in summer (Boyd et al., 1985; Dufois and Roualt, 2012; Jury, 1988; Largier et al., 1992). In this study, it can be seen that while the total upwelling velocities are less than that off Cape Hangklip, the dominant driver of upwelling at Danger Point is indeed wind stress curl induced Ekman pumping (Figure 4.10). The low contribution of BUI is likely due to the orientation of the coastline around Danger Point, as around the headland, the coastal orientation is not in the direction of either of the predominant wind directions, being south-easterly in summer and north-westerly in winter (Figure 4.2). Therefore, the orographic channelling of wind around the headland inducing wind stress curl is the main contribution to upwelling in this region (Boyd et al., 1985; Dufois and Roualt, 2012). Upwelling around Danger Point is therefore not represented in ERA5 as it is unable to capture small scale orography induced wind stress curl and resultant upwelling velocities.

Studies have shown that upwelling around Danger Point is less sensitive than that occurring off Cape Hangklip, and is therefore less strong or frequent (Jury, 1988), which is in agreement with the smaller magnitudes of upwelling presented in this thesis. As with the upwelling off Cape Hangklip, future work should study the spatial scale of the wind stress curl driven upwelling, and the sensitivity of this upwelling to the distance off the coast that it is calculated as well as identify whether upwelling at Danger Point is seen to this extent *in situ*, or whether other factors not included in this study are suppressing or enhancing upwelling in this region. Upwelling off Danger Point differs to that off Cape Point and Cape Hangklip in that the peak upwelling occurs to the east of the point, contrary to the literature which describes orography induced wind stress curl inducing upwelling to the west of capes (Nelson, 1981). While it is possible that this is due to a wind drop off at the coast east of Danger Point inducing negative wind stress curl, the exact mechanisms behind this are an interesting topic for future studies. In addition, further investigation of the non-rotational upwelling should be done as, while typically confined to within about a kilometre of the shore, it can be important in places like Danger Point where the wind blows offshore and northern shore of False Bay where wind blows onshore.

Upwelling on the WAB is understudied and of the previous studies, most are done in spring and summer as this is the upwelling season in the region (Largier et al., 1992). In the literature there are conflicting reports of when the maximum upwelling occurs, due to incomplete studies throughout the year. The results presented in this thesis show clear seasonal cycles in the identified upwelling regions of Cape Peninsula, Cape Hangklip and Danger Point, with the maximum upwelling occurring during January (Table 4.1, Figures 4.8-4.10).

While the identified upwelling regions show similar seasonal cycles, they differ in that the regions in the WAB, Cape Hangklip and Danger Point, show a stronger contribution of wind stress curl driven Ekman pumping to upwelling, relative to alongshore wind-driven BUI, than the Cape Peninsula upwelling cell. The lower BUI in these regions is likely due to, firstly; the change in orientation of the coastline in the WAB whereby, from Cape Point eastwards, the coastline transitions from a north-south orientated coastline typical of an EBUS to a more zonally oriented coastline (Figure 2.1), and secondly; the decrease in strength of wind stress that drives BUI upwelling (Figure 4.2). The higher contribution of wind stress curl induced

upwelling in the two identified regions on the WAB can be seen to be driven by the presence of a series of bays and capes more so than on the coastal region north of Cape Point, that produce strong wind stress curl driving Ekman pumping upwelling in summer. Previous work in the SBUS tends to simplify upwelling and place a larger emphasis on BUI upwelling as a result of alongshore wind stress, however the results presented in this thesis show that in some cases wind stress curl contributes more than double the contribution of BUI to upwelling, indicating that wind stress curl induced upwelling is key in the study of upwelling in this region (Largier, 2020).

It is again recommended that numerical ocean models using higher resolution winds, such as WASA3, are used to study the seasonal cycle in upwelling on the WAB, as with predicted changes in winds in the future, upwelling cycles over the WAB will likely change. The long-term southwards expansion/shift of the SAHP already being observed (Lamont et al., 2018) may result in stronger alongshore wind stress driving a higher contribution of BUI to upwelling, possibly creating stronger upwelling cells at Cape Hangklip, Danger Point and even Cape Agulhas. Lamont et al. (2018) found a significant increase in upwelling as a result of alongshore wind stress on the coastal region to the east of Cape Hangklip, indicating that the upwelling region of the SBUS may expand eastwards past Cape Agulhas with the southwards expansion of the SAHP. The effects this may have on wind stress curl driven upwelling are not clear, however it is possible that it may cause stronger winds over the WAB and a stronger wind drop off to the coast, thus inducing stronger negative wind stress curl and Ekman pumping upwelling in the region. In order to be able to predict possible future changes such as these, which have the potential to have major socio-ecological implications, current seasonality and upwelling dynamics need to be properly resolved in models, to allow for simulations of what may occur should the winds expand southwards.

6. Conclusion

Previous studies on the WAB are hindered by short durations, limited spatial extents and low-resolution wind products, with sparse *in situ* measurements to supplement knowledge on this region. This is the first complete high-resolution study of the WAB that allows for a continuous analysis of wind-driven upwelling along the coast and identification of the extent of regions of strong upwelling. It can be concluded that WASA3 is more suitable for upwelling studies in this region due to its higher resolution, however previous modelling studies have used wind products with a resolution comparable to that of ERA5. This highlights the need for ocean models to be developed and run for the WAB with high resolution wind products such as WASA3 to accurately simulate upwelling in this understudied region.

The WAB, from Cape Point to Cape Agulhas, is a unique, transitional region as it is located at the southern extent of one of the main EBUSs, with the influence of adjacent western boundary current, the Agulhas Current. This thesis has been one of the first studies in the region to highlight the importance of wind stress curl on wind-driven upwelling, and to identify regions where wind-driven upwelling should occur theoretically, being at Cape Hangklip and Danger Point. Despite this, large gaps in the knowledge of upwelling in the WAB remain, such as the influence of other factors on upwelling that are not taken into account in this study, including bathymetry and stratification, and how these affect the upwelling rates seen *in situ*. This study recommends that the next step to improving understanding of upwelling dynamics on the WAB is to use a numerical ocean model forced with a high-resolution wind product, such as WASA3, to simulate wind-driven upwelling as well as the effects of bathymetry and stratification. Ideally this would be validated with *in situ* measurements in upwelling cells in the region, however these are not available and thus this study further recommends the implementation of an *in situ* monitoring program in the WAB that will measure upwelling related variables, such as vertical velocity and temperature throughout the water column.

This region is of great socio-economic importance, given that it supports fisheries, aquaculture and eco-tourism. Upwelling is key in the productivity of this region as it allows

for water from depth to surface, bringing with it high concentrations of nutrients that support primary productivity. Some fisheries in this region are in decline, and with predicted and observed changes in upwelling in the region, there is the possibility that the socio-economic activities will be further under threat. The successful implementation of an ocean model in studying upwelling in this region will allow for simulations on long-term future changes in the region driven by the southward expansion/shift of the SAHP and allow for those dependent upon this region to implement mitigation measures for the predicted changes.

Reference List

Abrahams, A., Schlegel, R.W. and Smit, A.J., 2021. A novel approach to quantify metrics of upwelling intensity, frequency, and duration. *PLoS One*, 16(7), p.e0254026.

Andrews, W.R.H. and Hutchings, L., 1980. Upwelling in the southern Benguela Current. *Progress in Oceanography*, 9(1), pp.1-81.

Attwood, C.G. and Farquhar, M., 1999. Collapse of linefish stocks between Cape Hangklip and Walker Bay, South Africa. *South African Journal of Marine Science*, 21(1), pp.415-432.

Bakun, A., 1973. Coastal upwelling indices, west coast of North America, 1946-71.

Bang, N.D., 1973. Characteristics of an intense ocean frontal system in the upwell regime west of Cape Town. *Tellus*, 25(3), pp.256-265.

Bell, B., Hersbach, H., Simmons, A., Berrisford, P., Dahlgren, P., Horányi, A., Muñoz Sabater, J., Nicolas, J., Radu, R., Schepers, D. and Soci, C., 2021. The ERA5 global reanalysis: Preliminary extension to 1950. *Quarterly Journal of the Royal Meteorological Society*, 147(741), pp.4186-4227.

Bentamy, A., Grodsky, S.A., Cambon, G., Tandeo, P., Capet, X., Roy, C., Herbette, S. and Grouazel, A., 2021. Twenty-Seven years of scatterometer surface wind analysis over eastern boundary upwelling systems. *Remote Sensing*, 13(5), p.940.

Biastoch, A., Böning, C.W. and Lutjeharms, J.R.E., 2008. Agulhas leakage dynamics affects decadal variability in Atlantic overturning circulation. *Nature*, 456(7221), pp.489-492.

Boyd, A.J., Tromp, B.B.S. and Horstman, D.A., 1985. The hydrology off the South African south-western coast between Cape Point and Danger Point in 1975. *South African Journal of Marine Science*, 3(1), pp.145-168.

Capet, X.J., Marchesiello, P. and McWilliams, J.C., 2004. Upwelling response to coastal wind profiles. *Geophysical Research Letters*, 31(13).

Carr, M., Lamont, T. and Krug, M., 2021. Satellite sea surface temperature product comparison for the Southern African marine region. *Remote Sensing*, 13(7), p.1244.

Chapman, P. and* Largier, J.L., 1989. On the origin of Agulhas Bank bottom water. *South African Journal of Science*, 85(8), p.515.

Chavez, F.P. and Messié, M., 2009. A comparison of eastern boundary upwelling ecosystems. *Progress in Oceanography*, 83(1-4), pp.80-96.

Chavez, F.P., Sevadjian, J., Wahl, C., Friederich, J. and Friederich, G.E., 2018. Measurements of pCO2 and pH from an autonomous surface vehicle in a coastal upwelling system. *Deep Sea Research Part II: Topical Studies in Oceanography*, 151, pp.137-146.

Chelton, D.B., DeSzoeke, R.A., Schlax, M.G., El Naggar, K. and Siwertz, N., 1998. Geographical variability of the first baroclinic Rossby radius of deformation. *Journal of Physical Oceanography*, 28(3), pp.433-460.

Christensen, M.S., 1980. Sea-surface temperature charts for Southern Africa South of 260S. *South African Journal of Science*, 76(12), p.541.

Coleman, F., 2019. The development and validation of a hydrodynamic model of False Bay. M.Sc. Thesis. Stellenbosch University. Available at: http://scholar.sun.ac.za/handle/10019.1/106078 (Accessed: 8 November 2022).

Coleman, F., Diedericks, G.P.J., Theron, A.K. and Lencart e Silva, J., 2021. Three-dimensional modelling of the circulation in False Bay, South Africa. *African Journal of Marine Science*, 43(1), pp.95-118.

Cram, D.L., 1970. A suggested origin for the cold surface water in central False Bay. *Transactions of the Royal Society of South Africa*, 39(2), pp.129-137.

Desbiolles, F., Blanke, B., Bentamy, A. and Grima, N., 2014. Origin of fine-scale wind stress curl structures in the Benguela and Canary upwelling systems. *Journal of Geophysical Research: Oceans*, 119(11), pp.7931-7948.

Dufois, F. and Rouault, M., 2012. Sea surface temperature in False Bay (South Africa): Towards a better understanding of its seasonal and inter-annual variability. *Continental Shelf Research*, 43, pp.24-35.

Garzoli, S.L. and Gordon, A.L., 1996. Origins and variability of the Benguela Current. *Journal of Geophysical Research: Oceans*, 101(C1), pp.897-906.

GEBCO Compilation Group (2022) GEBCO 2022 Grid (doi:10.5285/e0f0bb80- ab44-2739-e053-6c86abc0289c).

Good, S., Fiedler, E., Mao, C., Martin, M.J., Maycock, A., Reid, R., Roberts-Jones, J., Searle, T., Waters, J., While, J. and Worsfold, M., 2020. The current configuration of the OSTIA system for operational production of foundation sea surface temperature and ice concentration analyses. *Remote Sensing*, 12(4), p.720.

Graham, W.M. and Largier, J.L., 1997. Upwelling shadows as nearshore retention sites: the example of northern Monterey Bay. *Continental Shelf Research*, 17(5), pp.509-532.

Hahmann, A., R. Floors, C. Lennard, D. Cavar, B. Olsen, N. Davis, N. Mortensen, and J. Hansen, 2021. Mesoscale and Microscale Downscaling for the Wind Atlas of South Africa (WASA) Project: Phase 3. Tech. Rep. E-0218, DTU Wind Energy, Denmark.

Hahmann, A.N., Pian, A., Lennard, C. and Mortensen, N.G., 2018. Mesoscale Modelling for the Wind Atlas of South Africa (WASA) Project–Phase II.

Hersbach, H., Bell, B., Berrisford, P., Hirahara, S., Horányi, A., Muñoz Sabater, J., Nicolas, J., Peubey, C., Radu, R., Schepers, D. and Simmons, A., 2020. The ERA5 global reanalysis. *Quarterly Journal of the Royal Meteorological Society*, 146(730), pp.1999-2049.

Hersbach, H., Bell, B., Berrisford, P., Biavati, G., Horányi, A., Muñoz Sabater, J., Nicolas, J., Peubey, C., Radu, R., Rozum, I., Schepers, D., Simmons, A., Soci, C., Dee, D., Thépaut, J-N., 2018. ERA5 hourly data on single levels from 1959 to present. Copernicus Climate Change Service (C3S) Climate Data Store (CDS), 10.24381/cds.adbb2d47

Hutchings, L., Van der Lingen, C.D., Shannon, L.J., Crawford, R.J.M., Verheye, H.M.S., Bartholomae, C.H., Van der Plas, A.K., Louw, D., Kreiner, A., Ostrowski, M. and Fidel, Q., 2009. The Benguela Current: An ecosystem of four components. *Progress in Oceanography*, 83(1-4), pp.15-32.

Jury, M.R., 1984. Wind shear and differential upwelling along the SW tip of Africa. Ph. D. Thesis. University of Cape Town.

Jury, M.R., 1988. A climatological mechanism for wind-driven upwelling near Walker Bay and Danger Point, South Africa. *South African Journal of Marine Science*, 6(1), pp.175-181.

Jury, M.R., 2020. Coastal gradients in False Bay, south of Cape Town: what insights can be gained from mesoscale reanalysis?. *Ocean Science*, 16(6), pp.1545-1557.

Lamont, T., García-Reyes, M., Bograd, S.J., Van Der Lingen, C.D. and Sydeman, W.J., 2018. Upwelling indices for comparative ecosystem studies: Variability in the Benguela Upwelling System. *Journal of Marine Systems*, 188, pp.3-16.

Largier, J.L., 2020. Upwelling bays: how coastal upwelling controls circulation, habitat, and productivity in bays. *Annual Review of Marine Science*, 12, pp.415-447.

Largier, J. L., Chapman, P., Peterson, W. T. & Swart, V. P., 1992. The western Agulhas Bank: circulation, stratification and ecology, *South African Journal of Marine Science*, 12:1, 319-339, DOI: 10.2989/02577619209504709

Lutjeharms, J.R.E. and Meeuwis, J.M., 1987. The extent and variability of South-East Atlantic upwelling. *South African Journal of Marine Science*, 5(1), pp.51-62.

Lutjeharms, J.R.E., Durgadoo, J.V. and Ansorge, I.J., 2007. Surface drift at the western edge of the Agulhas Bank. *South African Journal of Science*, 103(1-2), pp.63-67.

Nelson, G., 1981. Upwelling plumes. *Transactions of the Royal Society of South Africa*, 44(3), pp.303-308.

Nelson, G. and Hutchings, L., 1983. The Benguela upwelling area. *Progress in Oceanography*, 12(3), pp.333-356.

Nelson, G., Boyd, A.J., Agenbag, J.J. and Duncombe, C.M., 1998. An upwelling filament north-west of Cape Town, South Africa. *African Journal of Marine Science*, 19.

Nicholson, S.A., 2012. The circulation and thermal structure of False Bay: a process-oriented numerical modelling and observational study. M. Sc. Thesis. University of Cape Town.

Olauson, J., 2018. ERA5: The new champion of wind power modelling?. *Renewable energy*, 126, pp.322-331.

Pauly, D. and Christensen, V., 1995. Primary production required to sustain global fisheries. *Nature*, 374(6519), pp.255-257.

Pfaff, M.C., Logston, R.C., Raemaekers, S.J., Hermes, J.C., Blamey, L.K., Cawthra, H.C., Colenbrander, D.R., Crawford, R.J., Day, E., Du Plessis, N. and Elwen, S.H., 2019. A synthesis of three decades of socio-ecological change in False Bay, South Africa: setting the scene for multidisciplinary research and management. *Elementa: Science of the Anthropocene*, 7.

Philander, S.G.H. and Yoon, J.H., 1982. Eastern boundary currents and coastal upwelling. *Journal of Physical Oceanography*, 12(8), pp.862-879.

Pitcher, G.C., Brown, P.C. and Mitchell-Innes, B.A., 1992. Spatio-temporal variability of phytoplankton in the southern Benguela upwelling system. *South African Journal of Marine Science*, 12(1), pp.439-456.

Ponton, T.J., 2021. Investigating phytoplankton fluctuations and drum filter effectiveness on an abalone farm in Hermanus, South Africa. M. Sc. Thesis. University of the Western Cape.

Ragoasha, N., Herbette, S., Cambon, G., Veitch, J., Reason, C. and Roy, C., 2019. Lagrangian pathways in the southern Benguela upwelling system. *Journal of Marine Systems*, 195, pp.50-66.

Richter, I., 2015. Climate model biases in the eastern tropical oceans: Causes, impacts and ways forward. *Wiley Interdisciplinary Reviews: Climate Change*, 6(3), pp.345-358.

Rossi, V., López, C., Hernández-García, E., Sudre, J., Garçon, V. and Morel, Y., 2009. Surface mixing and biological activity in the four Eastern Boundary Upwelling Systems. *Nonlinear Processes in Geophysics*, 16(4), pp.557-568.

Russo, C.S., Veitch, J., Carr, M., Fearon, G. and Whittle, C., 2022. An intercomparison of global reanalysis products for Southern Africa's major oceanographic features. *Frontiers in Marine Science*.

Rykaczewski, R.R. and Checkley Jr, D.M., 2008. Influence of ocean winds on the pelagic ecosystem in upwelling regions. *Proceedings of the National Academy of Sciences*, 105(6), pp.1965-1970.

Shannon, L.V., 2001. 'Benguela current' in Steel, J.H., Thorpe, S.A. and Turekian, K.K. (eds.) *Ocean Currents*, pp.23-34.

Shannon, L.V. and Nelson, G., 1996. The Benguela: large scale features and processes and system variability. In: Wefer, G., Berger, W.H., Siedler, G., Webb, D.J. (Eds.), *The South Atlantic*. Springer-Verlag, Berlin, pp. 163-210.

Shillington, F.A., Reason, C.J.C., Rae, C.D., Florenchie, P. and Penven, P., 2006. 4 Large scale physical variability of the Benguela Current Large Marine Ecosystem (BCLME). *Large marine ecosystems* (Vol. 14, pp. 49-70). Elsevier.

Skamarock, W. C., J. B. Klemp, J. Dudhia, D. O. Gill, D. M. Barker, M. G Duda, X.-Y. Huang, W. Wang, and J. G. Powers, 2008: A Description of the Advanced Research WRF Version 3. NCAR Tech. Note NCAR/TN-475+STR, 113 pp. doi:10.5065/D68S4MVH

Small, R.J., Curchitser, E., Hedstrom, K., Kauffman, B. and Large, W.G., 2015. The Benguela upwelling system: Quantifying the sensitivity to resolution and coastal wind representation in a global climate model. *Journal of Climate*, 28(23), pp.9409-9432.

Strub, P.T. and James, C., 2022. Evaluation of Nearshore QuikSCAT 4.1 and ERA-5 Wind Stress and Wind Stress Curl Fields over Eastern Boundary Currents. *Remote Sensing*, 14(9), p.2251.

Tedesco, P., Gula, J., Ménesguen, C., Penven, P. and Krug, M., 2019. Generation of submesoscale frontal eddies in the Agulhas Current. *Journal of Geophysical Research: Oceans*, 124(11), pp.7606-7625.

Veitch, J., Penven, P., and Shillington, F., 2009. The Benguela: A laboratory for comparative modeling studies. *Prog. Oceanogr*. 83, 296–302. doi: 10.1016/j. pocean.2009.07.008

Wainman, C.K., Polito, A. and Nelson, G., 1987. Winds and subsurface currents in the False bay region, South Africa. *South African Journal of Marine Science*, 5(1), pp.337-346.

Appendix A: WASA3 and ERA5 wind stress climatologies

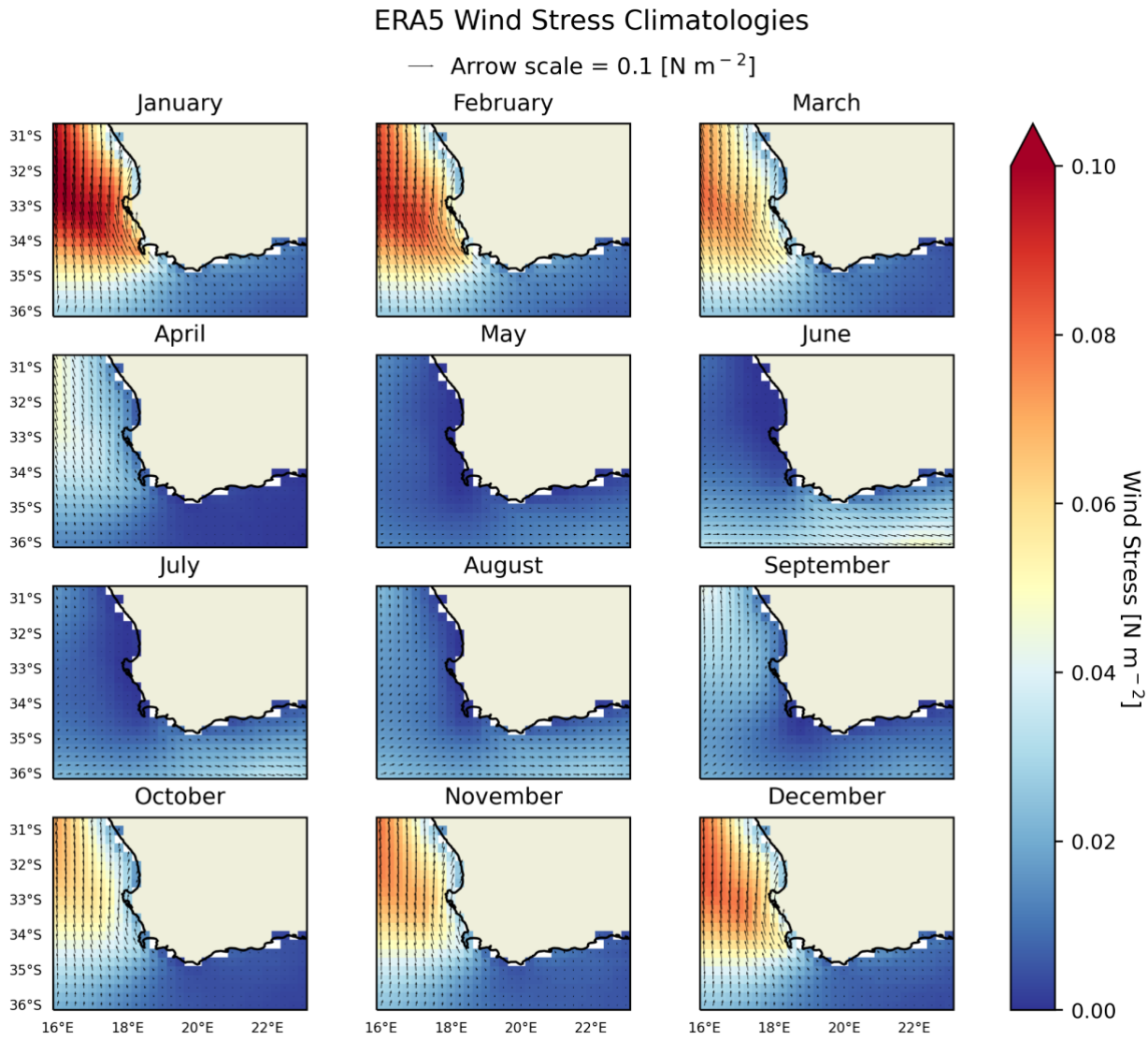

Figure A.1: ERA5 monthly wind stress climatologies from 1991 to 2019. Wind stress quivers have been plotted for every grid point in the ERA5 dataset, and every 7th grid point in the WASA3 dataset.

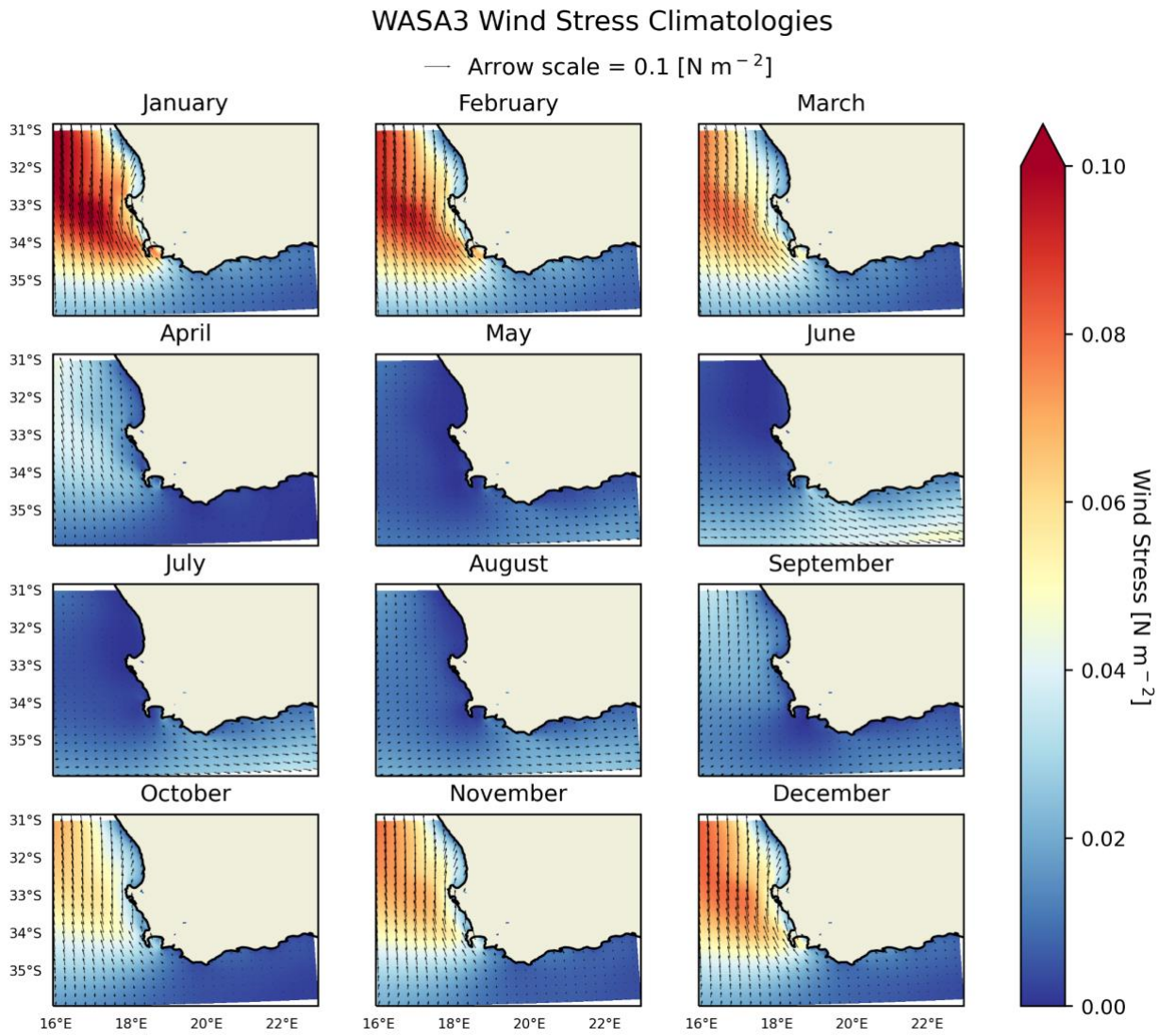

Figure A.2: WASA3 monthly wind stress climatologies from 1991 to 2019. Wind stress quivers have been plotted for every grid point in the ERA5 dataset, and every 7th grid point in the WASA3 dataset.